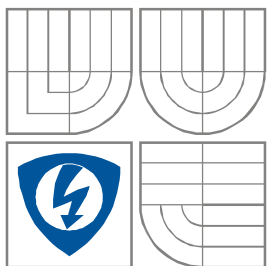


**VYSOKÉ UČENÍ TECHNICKÉ V BRNĚ**

BRNO UNIVERSITY OF TECHNOLOGY



**FAKULTA ELEKTROTECHNIKY A KOMUNIKAČNÍCH  
TECHNologií**

**ÚSTAV VÝKONOVÉ ELEKTROTECHNIKY  
A ELEKTRONIKY**

FACULTY OF ELECTRICAL ENGINEERING AND COMMUNICATION  
DEPARTMENT OF POWER ELECTRICAL AND ELECTRONIC  
ENGINEERING

## **SYNCHRONOUS GENERATOR REACTANCE PREDICITON USING FE ANALYSIS**

**VYPOCET REAKTANCÍ SYNCHRONIHO GENERATORU POMOCÍ METODY KONECNYCH PRVKU**

**DIPLOMOVA PRÁCE**

MASTER'S THESIS

**AUTOR PRÁCE**

AUTHOR

**Bc. Petr Chmelicek**

**VEDOUCÍ PRÁCE**

SUPERVISOR

**doc. Ing. Cestmir Ondrusek CSc.**

**BRNO, 2010**

## **Abstrakt**

Parametry náhradního obvodu synchronního stroje značně ovlivňují jeho chování jak při statickém provozu, tak především při náhlých dynamických jevech a poruchových stavech. Práce je zaměřena na zhodnocení dostupných metod pro výpočet těchto parametru pomocí Metody konečných prvků.

První část je věnována teoretickému popisu základních principů Metody konečných prvků a jejich aplikací na řešení problémů elektromagnetického pole v elektrických strojích. Zároveň také shrnuje základní uspořádání náhradního obvodu synchronního stroje, principy jeho konstrukce a základní funkci.

Druhá část je věnována praktickému výpočtu reaktancí náhradního obvodu synchronního stroje. S pomocí MKP jsou vypočteny synchronní reaktance s uvažováním vzájemného magnetického působení proudů v d a q ose. Pro výpočet transientních a subtransientních reaktancí jsou navrženy čtyři odlišné metody a jsou zhodnoceny z hlediska požadované přesnosti výpočtu a náročnosti na výpočetní čas.

Závěrečná část popisuje základní měřicí metody pro určení parametru náhradního obvodu na skutečném stroji. Kapitola také obsahuje srovnání simulace třífázového zkratu synchronního stroje s reálnou zkouškou provedenou laboratorně. Závěr obsahuje srovnání jednotlivých metod a návrh optimálního postupu pro výpočet zkoumaných parametrů.

## **Abstract**

Equivalent circuit parameters of synchronous machine greatly affects its performance during steady state operation and also during faults and transients. This thesis is focused on investigation and evaluation of different methods, for calculation of equivalent circuit parameters, based on the Finite Element Method.

First section gives theoretical overview of basic Finite Element Method principles and application on the magnetic field problems in electric machinery and fundamental concepts of synchronous machine operation and equivalent circuits, for different operation stages are discussed.

Second section is focused on identification of equivalent circuit parameters of four pole synchronous generator. Magneto-static FE simulation is used for calculation of synchronous reactances with cross coupling taken into account. For calculation of transient and subtransient parameters, four different methods are proposed and they are evaluated with respect to the accuracy and computation time.

Final section describes basic test procedures for synchronous machine equivalent circuit parameters estimation. Chapter also covers comparison of FE based simulation of dead short circuit at machine terminals and real test carried out in the laboratory. Summary gives a review of proposed methods and comparison of different approaches.

## **Klíčová slova**

Synchronní generator, metoda konečných prvků, reaktance, transientní analýza, magneto-statická analýza, časově harmonická analýza.

## **Keywords**

Synchronous generator, Finite element method, Reactance, Transient analysis, magneto-static analysis, time harmonic analysis.

## **Bibliografická citace**

Chmelicek, P. Synchronous generator reactance prediction using FE analysis, Brno: Vysoké učení Technické v Brně, Fakulta Elektrotechniky a Komunikačních Technologii, 2010. 62 s, Vedoucí diplomové práce doc.Ing. Cestmir Ondrusek, CSc.

## Prohlášení

Prohlašuji, že svou diplomovou práci na téma Synchronous generator reactance prediction using FE analysis jsem vypracoval samostatně pod vedením vedoucího diplomové práce a s použitím odborné literatury a dalších informačních zdrojů, které jsou všechny citovány v práci a uvedeny v seznamu literatury na konci práce.

Jako autor uvedené diplomové práce dále prohlašuji, že v souvislosti s vytvořením této diplomové práce jsem neporušil autorská práva třetích osob, zejména jsem nezasáhl nedovoleným způsobem do cizích autorských práv osobnostních a jsem si plně vědom následků porušení ustanovení § 11 a následujících autorského zákona č. 121/2000 Sb., včetně možných trestněprávních důsledků vyplývajících z ustanovení § 152 trestního zákona č. 140/1961 Sb.

V Brně dne .....

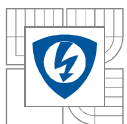
Podpis autora .....

## Poděkování

Děkuji vedoucímu diplomové práce Doc.Ing. Cestmiru Ondruskovi CSc. za účinnou metodickou, pedagogickou a odbornou pomoc a další cenné rady při zpracování mé diplomové práce.

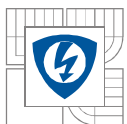
V Brně dne .....

Podpis autora .....



## CONTENTS

<b>1 INTRODUCTION.....</b>	<b>11</b>
<b>2 LITERATURE REVIEW.....</b>	<b>12</b>
<b>3 DESIGN OF ANALYZED MACHINE.....</b>	<b>14</b>
3.1 MAGNETIC CIRCUIT .....	15
3.2 WINDING CONFIGURATION .....	16
3.3 EXCITATION SYSTEM .....	18
3.4 AUTOMATIC VOLTAGE REGULATION .....	19
<b>4 SYNCHRONOUS MACHINE AND ITS EQUIVALENT CIRCUITS.....</b>	<b>20</b>
4.1 STEADY STATE OPERATION .....	20
4.2 OPERATION AT TRANSIENT AND SUBTRANSIENT STAGE .....	21
<b>5 BASIC CONCEPT OF FEM.....</b>	<b>25</b>
5.1 BOUNDARY CONDITIONS.....	26
5.2 MAGNETOSTATIC PROBLEMS.....	27
5.3 TIME HARMONIC PROBLEMS.....	28
5.4 TRANSIENT PROBLEMS .....	29
<b>6 IDENTIFICATION OF SYNCHRONOUS REACTANCE.....</b>	<b>30</b>
6.1 ANALYTICAL EXPRESSION OF SYNCHRONOUS REACTANCE.....	30
6.2 CALCULATION OF FLUX LINKAGE FROM FIELD SOLUTION .....	31
6.3 OPEN CIRCUIT CHARACTERISTIC .....	33
6.4 CALCULATION OF $X_d$ .....	34
6.5 CALCULATION OF $X_q$ .....	36
6.6 IMPACT OF CROSS COUPLING .....	38
6.7 CALCULATION OF END WINDING LEAKAGE REACTANCE.....	40
<b>7 IDENTIFICATION OF TRANSIENT AND SUBTRANSIENT REACTANCE.....</b>	<b>41</b>
7.1 MAGNETOSTATIC CALCULATION WITH MODIFIED BOUNDARY CONDITIONS .....	41
7.2 TIME HARMONIC SIMULATION.....	43
7.3 SINGLE FREQUENCY RESPONSE SIMULATION .....	44
7.4 SUDDEN SHORT CIRCUIT SIMULATION.....	46
<b>8 TESTING OF SYNCHRONOUS MACHINE.....</b>	<b>49</b>
8.1 SUDDEN THREE PHASE SHORT CIRCUIT TEST.....	49
8.2 TEST RESULTS AND SIMULATION RESULTS .....	52
<b>9 CONCLUSION.....</b>	<b>53</b>
<b>REFERENCES.....</b>	<b>56</b>
<b>SUPPLEMENT .....</b>	<b>58</b>



## LIST OF FIGURES

<i>Fig. 1- Operation principle of synchronous generator with brushless excitation system and automatic voltage regulator.....</i>	<i>14</i>
<i>Fig. 2- Magnetic circuit of the analyzed machine .....</i>	<i>15</i>
<i>Fig. 3- Winding configuration for one pole pitch. Solid line represents coil side placed in upper layer. ....</i>	<i>17</i>
<i>Fig. 4- Damper winding: Damper bars short circuited by end plates .....</i>	<i>17</i>
<i>Fig. 5- Rotating brushless excitation system .....</i>	<i>18</i>
<i>Fig. 6- Block diagram of typical Automatic Voltage regulator.....</i>	<i>19</i>
<i>Fig. 7- Simple salient pole synchronous machine .....</i>	<i>20</i>
<i>Fig. 8- Equivalent circuit of the salient pole synchronous machine at steady state.....</i>	<i>21</i>
<i>Fig. 9- Semi-logarithmic plot of peak current after the short circuit.....</i>	<i>22</i>
<i>Fig. 10-The path of armature reaction flux, denoted by red dashed line.....</i>	<i>22</i>
<i>Fig. 11- Equivalent reactances for q-axis .....</i>	<i>23</i>
<i>Fig. 12- Equivalent reactance for steady state, transient state and subtransient state.....</i>	<i>24</i>
<i>Fig. 13- Finite element mesh of two dimensional model of the synchronous generator.....</i>	<i>26</i>
<i>Fig. 14- Assignment of boundary conditions for simulation of synchronous machine.....</i>	<i>27</i>
<i>Fig. 15- Integration path for calculation of flux linkage from magnetic vector potential.....</i>	<i>32</i>
<i>Fig. 16- Output line to line voltage as a function of field current.....</i>	<i>33</i>
<i>Fig. 17- Winding configuration for calculation of d axis reactance .....</i>	<i>35</i>
<i>Fig. 18- Flux plot for armature winding excited by pure d axis current.....</i>	<i>35</i>
<i>Fig. 19- Impact of saturation on the values of synchronous reactance.....</i>	<i>36</i>
<i>Fig. 20- Winding configuration for calculation of d axis reactance .....</i>	<i>37</i>
<i>Fig. 21- Flux plot for armature winding excited by pure q axis current.....</i>	<i>37</i>
<i>Fig. 22- Flux plot for armature winding excited by armature current with d and q axis komponent .....</i>	<i>39</i>
<i>Fig. 23- D axis synchronous reactance as a function of d and q axis current in a form of contour plot.....</i>	<i>39</i>
<i>Fig. 24- Q axis synchronous reactance as a function of d and q axis current in a form of contour plot.....</i>	<i>40</i>

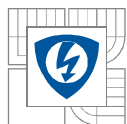
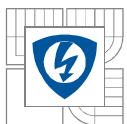


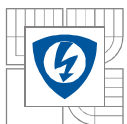
Fig. 25- Regions excluded from the FE model for A)transient conditions,B)subtransient conditions.....	41
Fig. 26- Flux plots for model with modified boundary conditions. A) transient condition, B) sub-transient conditions.....	42
Fig. 27- Transient and subtransient reactance profile computed by magneto static simulation with modified boundary conditions.....	42
Fig. 28- Flux plots for Time harmonic simulation for different frequency of injected current A) transient condition $f= 1\text{Hz}$ B) subtransient condition $f= 50\text{Hz}$ .....	43
Fig. 29- Comparison of direct axis reactances obtained by magneto static simulation and by time harmonic simulation.....	43
Fig. 30- Dependence of transient reactance profile on frequency of input current .....	44
Fig. 31- Setup for Single Frequency Response Test for: A) d axis subtransient reactance B) q axis subtransient reactance .....	44
Fig. 32- Winding distribution for simulation of Single frequency response. Rotor is aligned with nominal frequency a-phase and coils of b and c phase are in series and connected to source of AC voltage .....	45
Fig. 33- Flux plot for Single Frequency Response simulation in direct axis, contours show the induced current density in damper and field winding .....	45
Fig. 34- FE model of synchronous machine coupled with external electrical circuits for short circuit simulation .....	46
Fig. 35- Short circuit current trace with high-lighted peak values .....	47
Fig. 36- Simulated short circuit current traces .....	47
Fig. 37- Flux plots for Sudden Short Circuit simulation at different time instants after the three phase balanced short circuit, A) $t=0.005\text{s}$ , B) $t=0.055\text{s}$ , C) $t=0.195\text{s}$ . .....	48
Fig. 38- Extrapolation of transient and subtransient peak current.....	48
Fig. 39- Schematic diagram of sudden short circuit test.....	49
Fig. 40- Short circuit current traces during the sudden short circuit test.....	50
Fig. 41- Phase voltage waveform during the sudden short circuit test.....	50
Fig. 42- Rotor and exciter voltage during the sudden short circuit test.....	51
Fig. 43- Comparison of current traces from two independent Sudden Short Circuit tests .....	51
Fig. 44- Proposed simulation procedure for identification of all equivalent circuit parameters .....	54





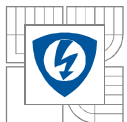
## LIST OF TABLES

<i>Tab. 1- Table of analyzed machine rating and parameters.....</i>	<i>15</i>
<i>Tab. 2- Armature winding parameters .....</i>	<i>16</i>
<i>Tab. 3- Table of results.....</i>	<i>52</i>

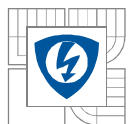


## SYMBOLS AND ABBREVIATIONS

$A_z$	Magnetic vector potential [ $\text{m}^2$ ]
$AVR$	Automatic voltage regulator
$B$	Magnetic flux density [T]
$\cos\varphi$	Power factor [-]
$D_g$	Air gap diameter [m]
$p$	Number of pole pairs
$PMG$	Permanent magnet generator
$R$	Resistivity [ $\Omega$ ]
$S$	Apparent power [kVA]
$H$	Magnetic field strength [A/m]
$H_c$	Coercive force [A/m]
$k_{ws1}$	Winding factor
$I$	Current [A]
$L_m$	Armature reaction inductance [H]
$J$	Current density [ $\text{A}/\text{mm}^2$ ]
$L_d$	Inductance in direct axis [H]
$L_q$	Inductance in direct axis [H]
$L_\sigma$	End winding leakage inductance [H]
$l$	Axial length of magnetic core [m]
$l_w$	Effective length of end winding [m]
$m$	Number of phases
$N_s$	Number of turns in series
$V$	Voltage [V]
$X_Q$	Q axis damper cage reactance [p.u.]
$X_D$	D axis damper cage reactance [p.u.]
$X_q$	Q axis synchronous reactance [p.u.]
$X_d$	D axis synchronous reactance [p.u.]
$X_m$	Magnetizing reactance [ $\Omega$ ]
$\vartheta$	Temperature [ $^\circ\text{C}$ ]



$Z$	Impedance [ $\Omega$ ]
$\Phi$	Magnetic flux [Wb]
$\gamma$	Permeance factor
$\alpha_B$	Temperature coefficient for remanence [%/°C]
$\alpha_H$	Temperature coefficient for coercive force [%/°C]
$\vartheta$	Electrical angle [rad], [°]
$\mu_0$	Permeability of vacuum [H/m]
$\mu_r$	Recoil permeability
$\xi$	Saliency ratio
$\Psi$	Flux linkage



# 1 INTRODUCTION

Reactances are parameters which greatly affect steady state and transient performance of synchronous generator, therefore precise identification of these parameters is critical task. In recent years there have been many advancements made in the art of synchronous machine reactance prediction. First attempts to identify these parameters were done by means of analytical formulations and tests. However, modern numerical methods allow electromagnetic field analysis of virtual prototypes based on actual geometry of the machine. This thesis is devoted to investigation of synchronous machine FE analysis for identification of steady state and transient parameters. Main target is to develop a procedure which will provide all characteristic parameters in both magnetic axis of the machine.

The finite element method is a numerical technique that is suitable for calculation of magnetic (in general any kind of field) field distribution over an analyzed domain. It allows a field solution to be obtained, even with time-variable fields and with non-linear material properties. It allows a good estimation of the performance and parameter of the electric machine under analysis. Due to the availability of powerful computing systems, FE method becomes a common tool of engineers and scientists. Computations in the thesis were carried out using Vector Fields Opera 2d and solvers for static, harmonic and transient problems.

First chapter deals with the literature review on a given topic. Accurate identification of equivalent circuit parameters is important task and lot of work has been done in this field during past decades, therefore there is large number of publications and textbooks covering the topic from different perspectives. Third chapter covers synchronous machine design with respect to the analyzed machine. Function of automatic voltage regulator and brushless excitation system is discussed and specific design properties of the generator set.

Mathematical modelling of synchronous machine is often based on two reaction theory and it employs several equivalent circuits. In fourth chapter a description of basic equivalent circuits of synchronous machine is given. Steady state and fault operation is considered and the physical explanation of phenomenon behind the transient and subtransient reactances. Following chapter is focused on description of basic concepts of Finite Element Method, applied to the field of electric machine analysis.

Sixth and seventh chapter represent the key part of the thesis, where the theoretical knowledge is applied to the practical problem. In the first section, the identification of synchronous reactance is discussed. The reactances are identified using non-linear magneto-static analysis, where impact of saturation and cross magnetization is taken into account. Computation of reactance is closely related to the computation of flux linkage, therefore this topic is discussed in detail. For identification of transient and subtransient reactances, four different methods are proposed and discussed. First two methods are special FE methods based on some simplifying assumptions, therefore time harmonic or even magneto-static solver may be used for analysis of naturally transient problem. Other two methods mimic standard test procedures.

The last chapters summarize results of simulations and compare them against test results. Optimal simulation procedure for identification of synchronous machine constants is proposed and possibility of future development is outlined.



## 2 LITERATURE REVIEW

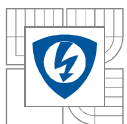
Traditionally, reactances are obtained from measurements on a real machine or calculated by means of analytical equations based on geometrical properties of the machine. However, a lot of work has been devoted to prediction of these parameters by computer aided simulations in recent years. Key role in these simulations plays the Finite Element Method and this thesis is devoted to investigation of different methodologies based on FE analysis. However, some analytical expressions may be useful for better understanding the problem. The numerical approach is very popular in recent years due to the availability of powerful computing systems, and due to the fact that numerical analysis can better evaluate impact of nonlinearities and other non-ideal properties of analyzed machine. On the other hand, analytical method allows development of fast and easy to use calculation tools for rough but instant parameter estimation.

[1] Offers good source of information on FE analysis of electrical machines and electromechanical devices in general. Methods and techniques described in the book are particularly oriented on calculations with use of planar and axial symmetry and three dimensional effects are mostly neglected or calculated separately by analytical equations. The book contains overview of electromagnetic field fundamentals and mathematical concepts of finite element method. Attention is also paid to techniques of main parameters identification for permanent synchronous machines. Theoretical knowledge is supported by results of real-life industrial problems and automated calculation algorithms are proposed. The book covers basic procedures for synchronous reactance calculation and even cross coupling effect is considered. Unfortunately, the book doesn't describe transient operation of synchronous machine.

[3] and [4] give exhaustive theoretical description of synchronous machine operation during steady state and transients. Books also cover mathematical modeling of the machine and concepts of equivalent circuits for different purposes and regimes of operation. Together with [2] offer great reference for analytical calculations and for better understanding of the synchronous machine modeling. The whole chapter in [3] is devoted to various test procedures for synchronous machines. Different methods are described in detail and it is concluded that for identification of transient and subtransient parameters, either sudden short circuit test or steady state frequency response test may be employed.

Method for calculation of transient and subtransient reactance with static FE simulation is given in [10]. This method employs equivalent magneto static model in which the unknown currents, induced in damper cage and field winding, are replaced by equivalent boundary condition. Because of this, regions with induced currents may be excluded from the FE model. Stator winding may be fed in order to get maximum of the MMF aligned with d or q axis, thus method allows calculation of reactances in both axis. Authors used proposed method in analysis of large salient pole hydro alternator and concluded good agreement with test results. Main advantages of this method should be simple FE model, short computation time and easy post processing of field solution.

In [13] authors calculated of reactances of synchronous machine with cylindrical rotor. Synchronous reactances were calculated by from the results of magneto static simulation with direct or quadrature axis aligned with a-phase axis and winding is fed by pure d or q axis current. Flux linkage for reactance calculation is obtained from distribution of magnetic vector potential in stator slots. Transient and subtransient reactances were analyzed separately for saturated and unsaturated conditions. For unsaturated regime authors used time harmonic simulation with linear material properties and static rotor. Subtransient and



transient stage is distinguished by absence of rotor iron conductivity in case of transient operation. Impact of different frequencies of injected current was investigated and it was concluded that for simulation of subtransient regime, higher frequency has to be used. Impact of saturation was taken into account by the same procedure used in [10]. Authors compared simulation results against test results and concluded that maximal error of numerical method is within ten percent range.

In [12] is presented calculation of reactances for salient synchronous machine equipped with damper winding. Synchronous reactances are calculated by well known method described in [1]. Investigation of transient and subtransient reactances was done by time harmonic simulation with locked rotor. Procedure is similar to method described in [13]. The main difference between these two methods is that authors in [13] assumed zero conductivity of rotor iron during transient stage but in this case transient and subtransient regime was distinguished by different frequency of supplied current. It was assumed that typical values of frequency for this simulation are one hertz for transient and fifty hertz for subtransient condition. Same approach is given in [2], but author warns that the results of this method strongly depend on appropriate choice of injected current frequency, which is main disadvantage.

Methods, for calculation of transient and subtransient reactance, described in above mentioned papers are special FE methods based on number of simplifying assumptions. According to [11] and [14] it is possible to mimic actual test procedure by time stepping simulation. Initially, machine runs with open circuited terminals and three phase balanced short circuit is applied at chosen time instant. Short circuit current traces are recorded and post-processed according to IEEE standards. Papers depict how to set the simulation and how to use external electric circuits coupled with electromagnetic solver. Papers show very good agreement between test and simulation results, however, accuracy of the procedure depends on precise knowledge of external circuit parameters, such as phase resistance and especially end winding leakage reactance. Short circuit test also doesn't produce parameters in quadrature axis thus this has to be identified separately by different simulation.

Another standard test procedure for estimation of synchronous machine reactances is Stand Still Frequency Response test. There are several advantages against classical short circuit test one of which is possibility of calculation q axis parameters. [15] describes the procedure in detail and proposes several improvements of the standard method. Rotor is locked in direct or quadrature position during the test and armature winding is fed from the AC voltage source with variable frequency and the input voltage, stator current, field current and phase lags are measured in a wide range of frequencies. Authors came to the conclusion, that steady state frequency response test is feasible for testing and modeling of synchronous machine with advantage of no risk of damage to the tested machine.

Traditional way of obtaining machine parameters is done by testing of the machine. Various test procedures and their detailed description is given in [7]. Proposed methods comply with IEEE standards and are widely used in industry and verified by many test on actual machines. Paper is divided in several parts and each one is devoted to certain aspect of synchronous machine testing. First part reviews basic concepts and discuss practical considerations of test methods. Second part describes the methods of determining the most important parameters and finally the third part illustrates the application of these methods to actual power machinery and presents tabulated test results as well as a table of typical constants. The appendixes summarize additional test methods and conclusions.

### 3 DESIGN OF ANALYZED MACHINE

Synchronous generators are the workhorse of the electrical power generation industry. Aim of this chapter is to summarize a basic concept of synchronous machine with respect to the analyzed machine, which is salient pole generator used in power generation set coupled with diesel engine.

All generators in general consist of two main parts termed the stator and the rotor, both of which are manufactured from laminated magnetic steel. The stator winding, also called armature winding, which carries the load current and supplies the current to the system, is placed in slots on the inner surface of the stator. Armature winding consists of three symmetrical phases. Rotor of synchronous machine is either cylindrical or salient pole but analyzed machine employs rotor with four salient poles on which the DC field winding is wound. The field winding is the main source of magnetic flux in the synchronous machine. The rotor also has additional rotor circuit in a form of aluminium bars placed in slots near the pole face area. This winding is called damper winding or amortisseur and its purpose is to damp mechanical oscillations of the rotor during sudden changes in load or during faults. This damper is made the same way as the squirrel cage of induction motor and is also short circuited by end-rings or end- plates.

The rotor excitation winding is supplied with a direct current to produce a rotating magnetic flux with the strength proportional to the excitation current. This rotating magnetic flux induces voltage across the three phase armature winding and as a result of this alternating currents flow to the power system. Another effect of the currents in the armature winding is to create their own magnetic field rotating with the same speed as the rotor. Resultant flux is stationary with respect to the rotor but rotates with respect to the stator. Due to this fact the stator has to be made of laminated magnetic steel, in order to suppress the impact of eddy current losses. Rotor is also made of same laminations, in case of analyzed machine, but it isn't strictly necessary.

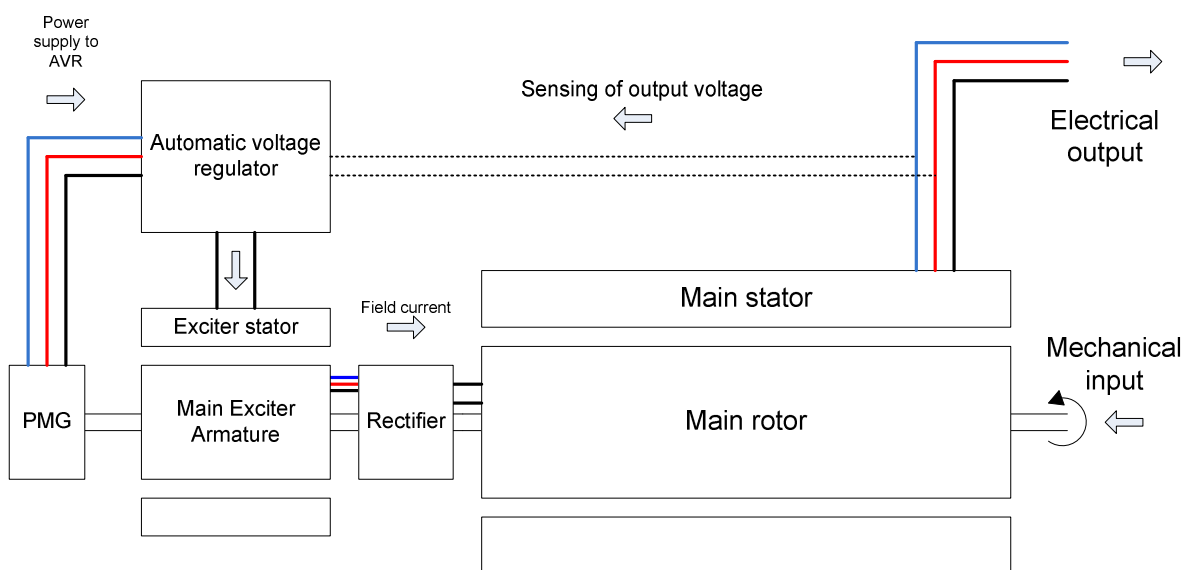


Fig. 1- Operation principle of synchronous generator with brushless excitation system and automatic voltage regulator

Damper winding enhances the dynamic behaviour of synchronous machine. If the speed deviated from synchronous, the relative speed of rotor and the speed of resultant magnetic field become different and as a result the currents are induced in the damper winding. These currents will oppose the flux change that has produced them and helps to stabilise the synchronous speed of the rotor.

Figure () shows the block diagram of typical generator set with its main components and relationships between them. Typical generator set consists of diesel engine with its shaft coupled with the shaft of synchronous generator. On the main generator shaft is also a brushless excitation system. In case of analyzed machine this excitation system consist of two smaller generators purpose of which is to supply electrical energy to automatic voltage regulator and to main excitation winding of the machine via the uncontrolled rectifier. Generator is usually connected to the grid via step up transformer. Relevant parts of the generator set will be described in the following chapters.

Rated power [kVA]	1400
Rated voltage [V]	380
Number of poles	4
Rated speed [rpm]	1500
Rated power factor	0.8
Rated efficiency [%]	96
Frequency [Hz]	50

Tab. 1- Table of analyzed machine rating and parameters

### 3.1 Magnetic circuit

Magnetic circuit of the analyzed machine is made of steel laminations of M470-65 grade. Stator has sixty round shaped slots, prepared for double layer winding. Rotor has four salient poles with uniform air gap along the pole face area. Each pole has eight circular slots, for damper bars, near the pole face and additional two slots for steel bars, which mechanically support the field winding against centrifugal forces.

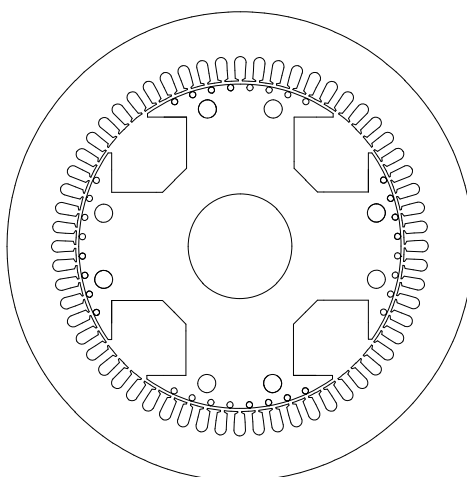
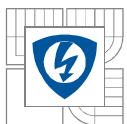


Fig. 2- Magnetic circuit of the analyzed machine





### 3.2 Winding configuration

As was mentioned before, operating principle of synchronous machine is based on interaction between magnetic fields and the currents flowing in the winding. The analyzed machine employs three windings:

1. Stator three phase armature winding – Armature winding delivers active power from the generator to the connected load.
2. Rotor field winding – Field or magnetizing winding creates main magnetic field of the machine. It is fed by direct current through the carbon brushes and slip rings or through the brushless excitation system.
3. Damper winding – Damper winding is active during transient operation of the machine. It damps the fluctuations of the rotation speed caused by pulsating torque loads.

Armature winding of analyzed machine is double layer lap winding, which means that each stator slot contains two coil sides. Winding is short pitched and has a step of two thirds of the full coil step. Short pitching influences the harmonics content of the flux density of the air gap. A correctly short-pitched winding produces a more sinusoidal magneto motive force distribution than a full-pitch winding. In a salient-pole synchronous generator, where the flux density distribution is basically governed by the shape of pole shoes, a short-pitch winding produces a more sinusoidal pole voltage than a full-pitch winding []. Also copper consumption is reduced as a result of short pitching. Tab.1 shows main parameters of the armature winding and fig.4 shows winding configuration diagram.

Number of poles	4
Number of layers	2
Number of stator slots	60
Coil groups	10
Coils per group	12
Coil pitch	5
Short pitching	two thirds
Turns per coil	2
Parallel paths	4
Slot fill factor [%]	77.4
Phase resistance [ $\Omega$ ]	0.00126
Core length [mm]	550
End winding length [mm]	147
Conductor diameter [mm]	2

Tab. 2- Armature winding parameters

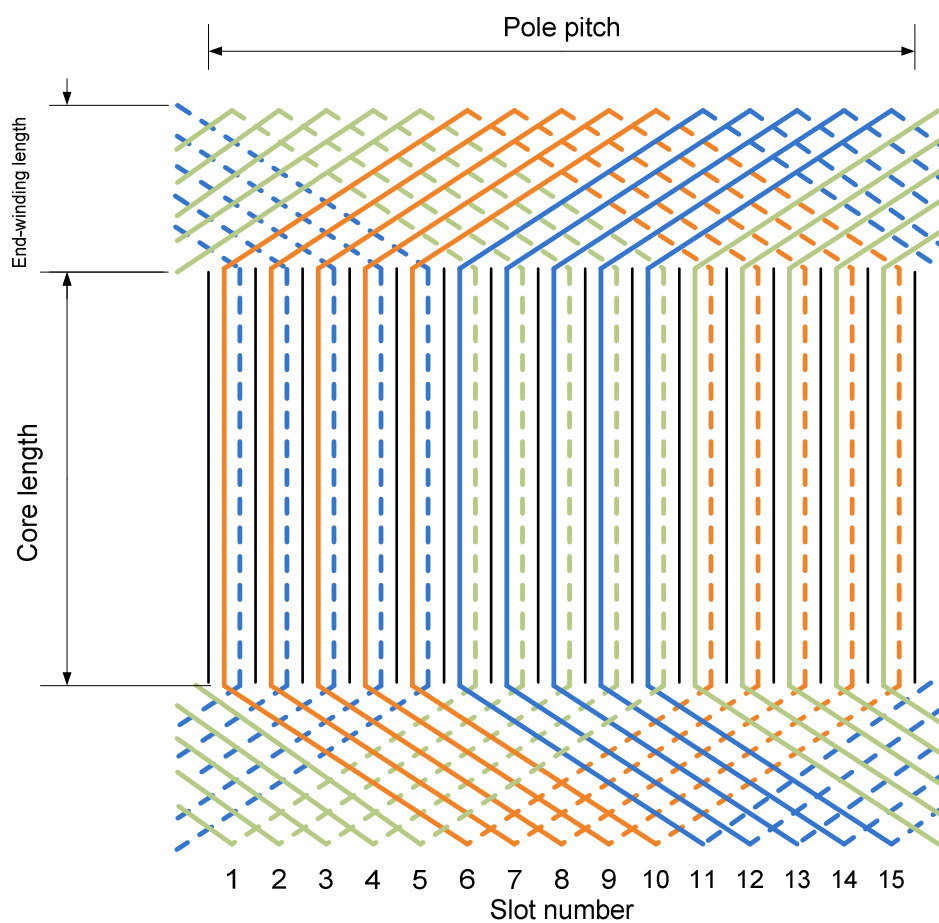


Fig. 3- Winding configuration for one pole pitch. Solid line represents coil side placed in upper layer.

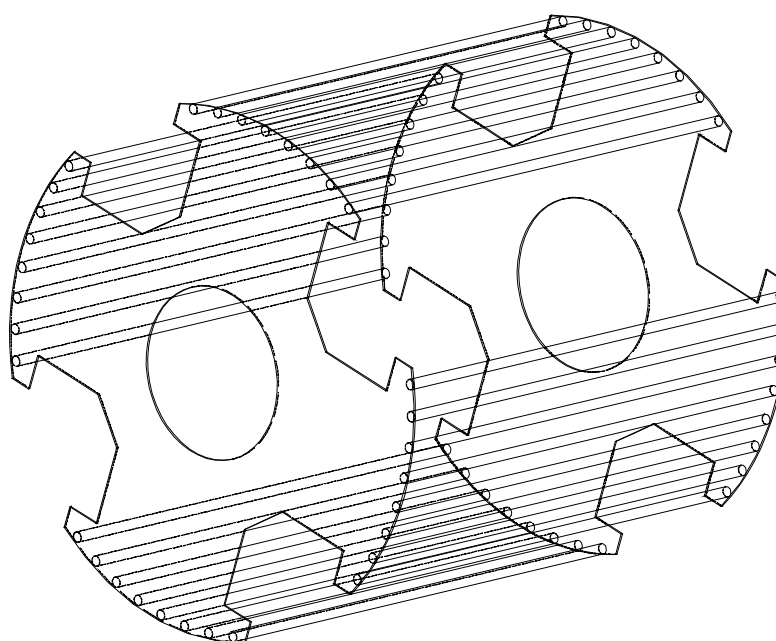


Fig. 4- Damper winding: Damper bars short circuited by end plates

### 3.3 Excitation system

Purpose of excitation system is to supply main field winding on the rotor of synchronous machine with DC current and this system is usually controlled by automatic voltage regulator. Analyzed machine is equipped with brushless rotating exciter and with additional auxiliary permanent magnet generator as a main supply of automatic voltage regulator.

The brushless rotating exciter is a small inside-out synchronous generator with its field winding mounted on the stator and its armature circuit mounted on the rotor shaft. The three phase output of the exciter generator is rectified to direct current by a 3-phase rectifier circuit also mounted on the shaft of the generator, and is then fed to the main dc field winding. By controlling the small dc field current of the exciter generator (located on the stator), we can adjust the field current on the main machine without necessity to use slip rings and brushes. For operation of generator set without external source of electrical energy, self excitation is required. Magnetic circuit of the rotating exciter has to be made of laminations with high residual magnetism, thus producing magnetic flux even with zero excitation current.

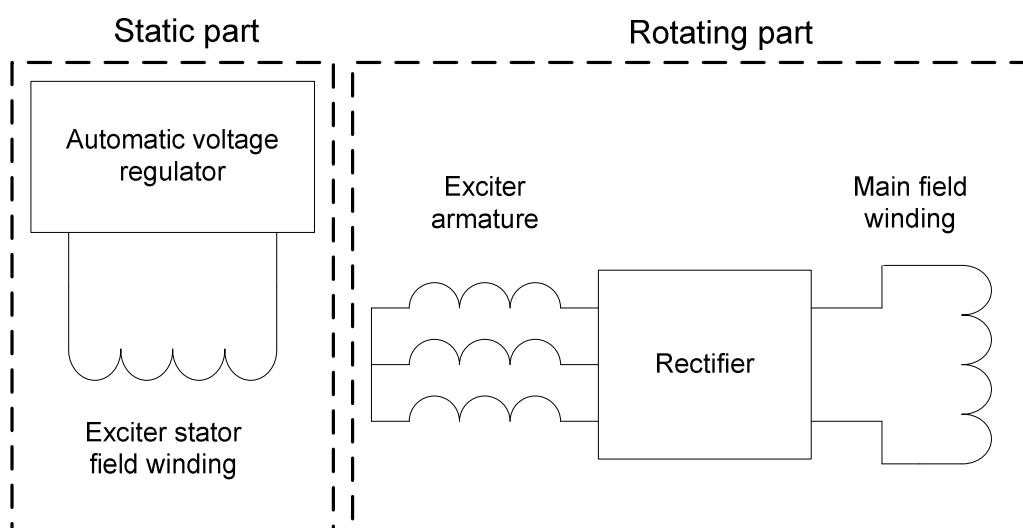


Fig. 5- Rotating brushless excitation system

To make the excitation of the generator reliable and completely independent of any external power sources, another smaller exciter is mounted on the main shaft. This smaller exciter is a permanent magnet synchronous machine where permanent magnets are placed on the rotor (or embedded in the rotor structure) and they are the main source of magnetic flux for this machine. The PMG gives a constant output power for excitation winding of the main exciter and the whole generator set is completely independent of any external source of electric energy. Excitation current is generated by small PMG and then amplified by main exciter and through the rectifier delivered to the main field winding. To control the input of main exciter, automatic voltage regulator is connected between the PMG and the main exciter field winding. One limitation of this type of exciter is that field current can be controlled only indirectly by field control of exciter which brings time constant of the machine into excitation control system. Main exciter is designed with higher number of poles than main machine so that the output voltage has higher frequency.

Because there is no mechanical contact between rotor and stator, brushless excitation system doesn't require periodical maintenance, as and it's widely used in modern generators.

### 3.4 Automatic voltage regulation

Automatic voltage regulator regulates the terminal voltage of the generator by controlling the amount of current supplied to the generator field winding by the exciter. The AVR measures the output voltage and compare it with reference value. Difference between measured value and reference value is then used for altering of exciter output to minimize this difference. This represents the negative feedback loop control of output voltage. Block diagram of typical voltage regulator components is shown on Fig.6.

The AVR subsystem also includes a number of limiters whose function is to protect the AVR, exciter and generator from excessive voltages and currents. They do this by maintaining the AVR signals between preset limits. Thus the amplifier is protected against excessively high input signals, the exciter and the generator against too high a field current, and the generator against too high armature current and too high power angle. AVR control systems depend upon voltage feedback from the generator terminals, to control the output voltage. If the sensed input signal is too low, it tries to increase the feedback signal to nominal value, which can result in high voltage output at the generator terminals thus there has to be an overvoltage protection system. The last three limiters have built-in time delays to reflect the thermal time constant associated with the temperature rise in the winding [].

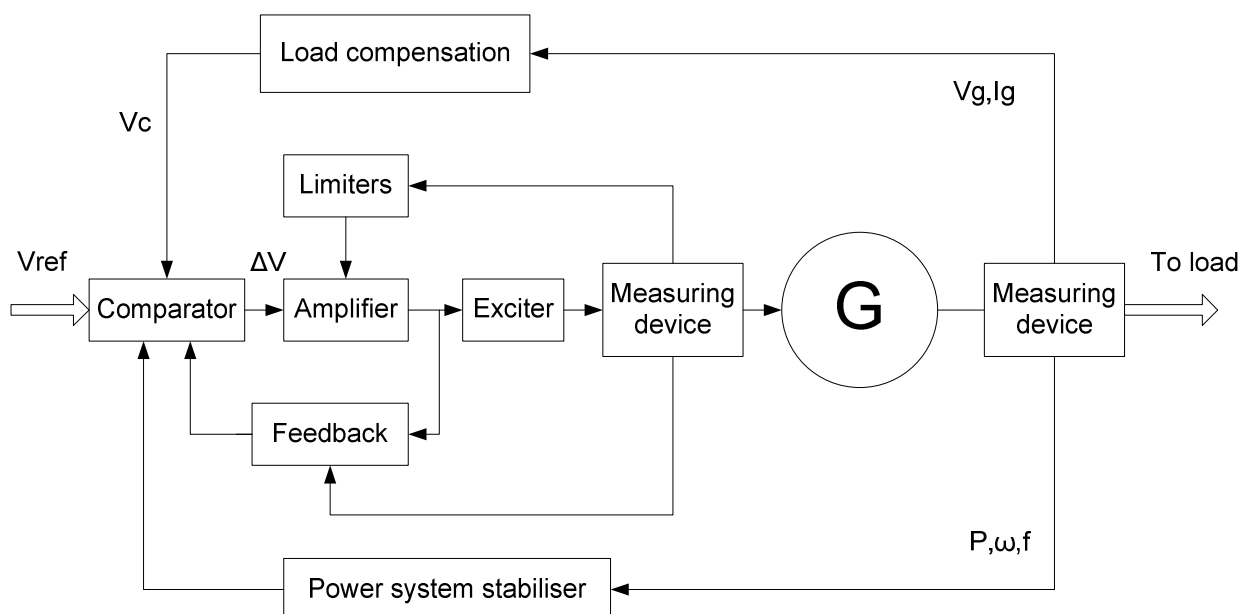


Fig. 6- Block diagram of typical Automatic Voltage regulator

Load compensation system together with comparator maintains constant output voltage under different load conditions and power system stabiliser helps to damp power swings in the power system.

## 4 SYNCHRONOUS MACHINE AND ITS EQUIVALENT CIRCUITS

Purpose of the following sections is to give a brief overview of different equivalent circuits used for simulation and analysis of synchronous machine and their relation to different stages of a synchronous machine operation.

### 4.1 Steady state operation

In general, salient pole synchronous machine in steady state can be represented by simplified schematic diagram, such as one on Fig.4. The machine on the figure has four coils. The beginning and end of coil representing field winding is denoted by  $f1$  and  $f2$  respectively, while the beginning and end of each of the phase windings are denoted by letter corresponding to the phase, for example  $a1$  is the beginning and  $a2$  is end of a-phase coil. The stator has three axis  $a, b$  and  $c$ , each corresponding to one of the phase windings. The rotor has two axis: the direct axis, which is the main magnetic axis of the field winding and the quadrature axis, ninety electrical degrees displaced with respect to the direct axis.

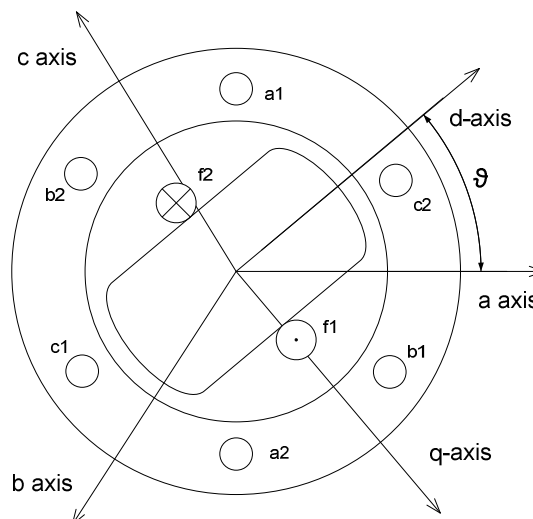


Fig. 7- Simple salient pole synchronous machine

The main problem with modelling of salient pole machine is that the width of the air gap varies circumferentially around the generator with the narrowest gap being along direct axis and the widest along the quadrature axis. It is obvious that the flux in quadrature axis has to overcome much higher reluctance than in case of d axis thus air gap reluctance varies between these two extreme values and thanks to that, stator phase reactance depend on the rotor position. A common technique in salient synchronous machine analysis is to resolve the machine quantities into rotor reference d-q frame, which rotates at the same speed as rotor. Three phase armature winding is replaced by two equivalent windings, one along d-axis is and other one along q axis. These two equivalent armature windings are assumed to rotate with the rotor at synchronous speed. This makes analysis of salient pole machine much easier and it can be done by well known d-q transformation in which the stator quantities are multiplied by coefficients of transformation matrix. Transformation of stator currents into d-q reference frame is shown by equation (). This equation assumes steady state balanced conditions thus zero sequence is not present in the equation.

$$\begin{bmatrix} I_d \\ I_q \end{bmatrix} = \begin{bmatrix} \cos(\vartheta) & \cos(\vartheta - 2\pi/3) & \cos(\vartheta + 2\pi/3) \\ \sin(\vartheta) & \sin(\vartheta - 2\pi/3) & \sin(\vartheta + 2\pi/3) \end{bmatrix} \cdot \begin{bmatrix} I_a \\ I_b \\ I_c \end{bmatrix} \quad (1.1)$$

Where a,b and c are stator quantities and d,q are synchronous rotating reference frame quantities,  $\vartheta$  is angular displacement between direct and a-phase axis. Voltage equations for equivalent armature winding may be written as follows:

$$\begin{aligned} V_d &= R_s I_d + X_d I_d - \omega \psi_q \\ V_q &= R_s I_q + X_q I_q + \omega \psi_d \end{aligned} \quad (1.2)$$

Where  $R_s$  is stator phase resistance,  $V_d$  and  $V_q$  are equivalent stator voltages,  $I_d$  and  $I_q$  equivalent stator currents,  $\omega \Psi$  is induced voltage by q and d axis flux respectively,  $X_d$  and  $X_q$  are synchronous reactances independent on the rotor position. Precise identification of these reactances is one of the main tasks of this thesis and it will be described in detail in following chapters.

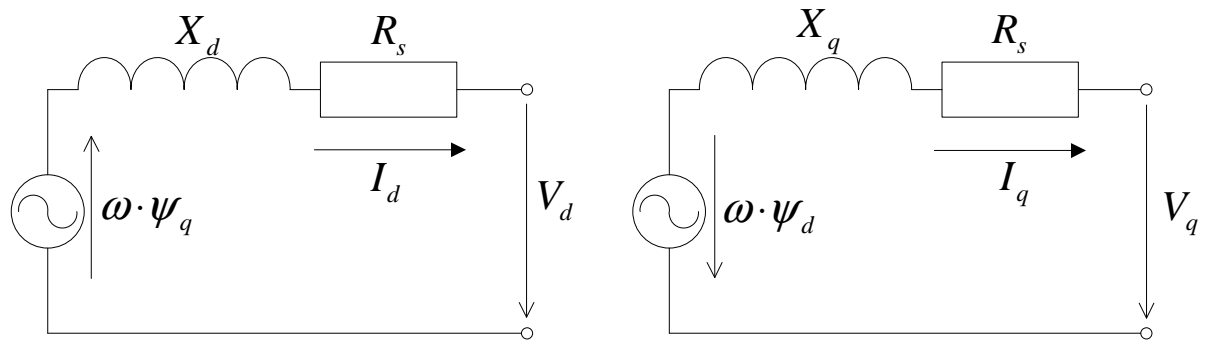


Fig. 8- Equivalent circuit of the salient pole synchronous machine at steady state

Synchronous reactance consists of two parts. First component is called magnetizing reactance, which is reactance related to the main flux path. Second component is related to the reluctance of leakage paths. Both components are calculated separately by means of analytical formulation, but FE procedure gives the resultant value, thus these components won't be treated separately. According to the voltage equations given in (1.2), the steady state equivalent circuit for direct and quadrature axis may be constructed.

## 4.2 Operation at transient and subtransient stage

Previous section describes general equivalent circuit of salient pole synchronous machine during steady state operation. This stage is modelled by two separate circuits, each for corresponding axis, with source of induced voltage, phase resistance and synchronous reactance connected in series. Similar approach may be adopted for description of transient and subtransient regimes, but with different value of reactance because currents induced in field and damper winding force the armature flux to take a different path to that in the steady state. As the currents in the rotor circuit prevent the armature reaction flux from passing through the rotor winding, they have the effect of screening the rotor from these changes in armature flux[6].

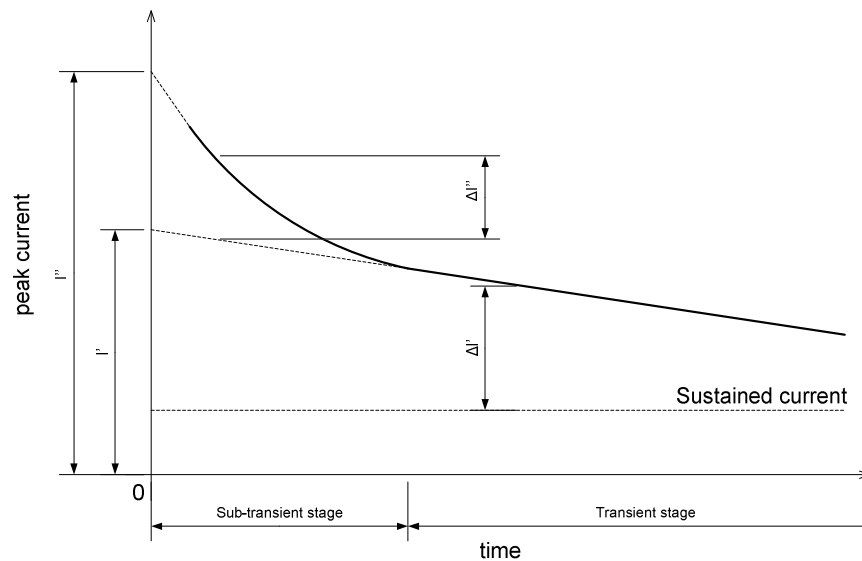


Fig. 9- Semi-logarithmic plot of peak current after the short circuit

Three different stages of screening are usually distinguished and Fig. 10 shows three different armature reaction flux paths. Immediately after the short circuit at the machine terminals occurs, the current is induced in both the damper and field winding and it forces the armature reaction flux completely out of the rotor to keep the rotor flux linkage constant. This stage is called subtransient and it is showed on figure (c). As energy is dissipated in the resistance of the rotor windings, the currents maintaining constant rotor flux linkages decay with time allowing flux to enter the windings. As the rotor damper winding resistance is the largest, the damper current is the first to decay, allowing the armature flux to enter the rotor pole face. However, it is still forced out of the field winding itself, Figure 4.8b, and the generator is said to be in the *transient state*. The field current then decays with time to its steady-state value allowing the armature reaction flux eventually to enter the whole rotor and assume the minimum reluctance path. This steady state is illustrated in Figure 4.8c and corresponds to the flux path shown in the top diagram of [Figure 4.5b](#).[]

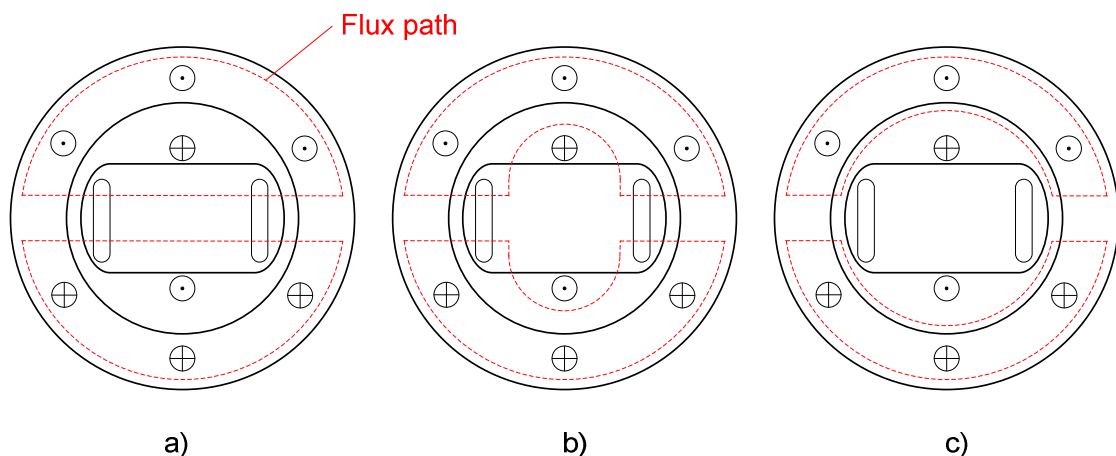


Fig. 10-The path of armature reaction flux, denoted by red dashed line

It is obvious, that following a fault synchronous generator becomes a dynamic source that has time dependent reactance and internal voltage. Rather than considering one generator model with time dependant reactance and induced voltage, it is more suitable to divide the generator response into three stages. Each of these stages is analyzed separately and different equivalent circuit is assigned for steady state, transient and subtransient state. In each of the characteristic states, the generator may be modelled by the source of constant induced voltage behind a constant reactance. The reactance of a winding is defined as the ratio of the flux linkage of the winding to the current which creates the flux linkage, multiplied by angular velocity. From the Fig.10 is apparent that the flux path is almost entirely in air and so the reluctance of this path is very high. In contrast, the flux path in the steady state is closed through the rotor iron with much lower reluctance. Consequently, the transient and subtransient reactances are significantly lower than synchronous reactance. Total reactance may be decomposed in number of separately analyzed reactances, each of which pertains to a specific part of the flux path. The equivalent reactance circuit for each characteristic stage is given in fig.11 and fig.12.

Steady state, transient and subtransient reactance in direct axis are defined as a parallel combination of magnetizing reactance  $X_{md}$ , armature leakage reactance  $X_{ro}$ , field winding reactance  $X_f$  and damper cage reactance  $X_D$ .

$$\begin{aligned} X_d &= X_{\sigma} + X_{md} \\ X'_d &= X_{\sigma} + \frac{1}{\frac{1}{X_{md}} + \frac{1}{X_f}} \\ X''_d &= X_{\sigma} + \frac{1}{\frac{1}{X_{md}} + \frac{1}{X_f} + \frac{1}{X_D}} \end{aligned} \quad (1.3)$$

When the short circuit is applied during the no-load operation of the generator, peak value of magneto-motive force is aligned along the direct axis and q-axis component equals zero. If the fault occurs on loaded generator, the MMF has both components thus it is necessary to analyse effect of two armature MMFs separately using the two reaction theory described in section about steady state operation.

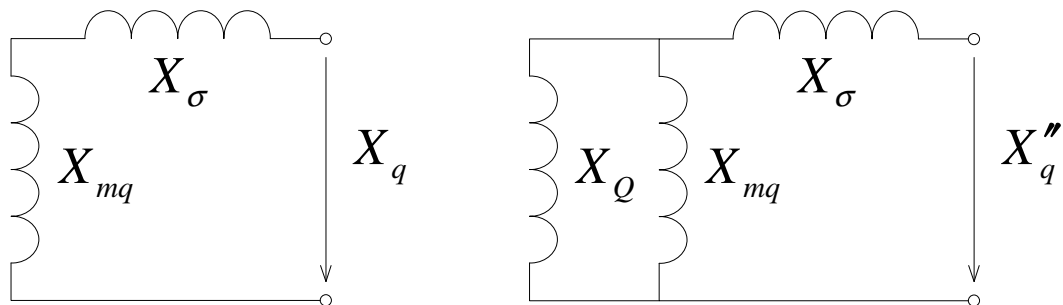


Fig. 11- Equivalent reactances for q-axis



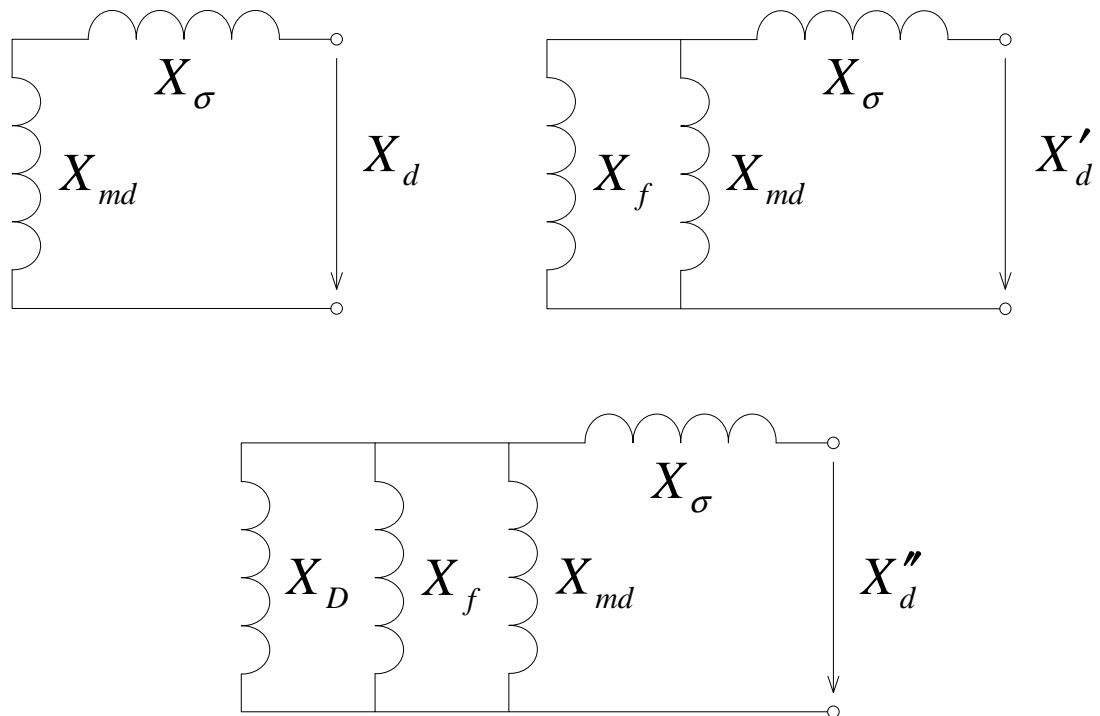


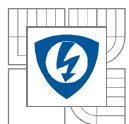
Fig. 12- Equivalent reactance for steady state, transient state and subtransient state

If the armature MMF is aligned along quadrature axis, the only currents preventing the armature reaction flux from passing through the rotor iron are currents induced in q-axis part of the damper winding, because field winding is placed in direct axis only. Due to this fact, it may be assumed, that q-axis transient reactance equals magnetizing reactance and only two equivalent reactances are defined.

$$X_q = X_\sigma + X_{mq}$$

$$X'_q = X_\sigma + \frac{1}{\frac{1}{X_{mq}} + \frac{1}{X_D}} \quad (1.4)$$

Decomposition of resultant reactances into individual components is especially useful for analytical calculations and gives good understanding of the physical phenomenon behind dynamic operation of synchronous machine. However, resultant values may be computed directly from the FE simulation without necessity to calculate the components separately.



## 5 BASIC CONCEPT OF FEM

The Finite Element method is used to obtain solutions to partial differential or integral equations that cannot be solved by analytic methods. With availability of powerful computers the Finite Element Method became a common tool for scientists and engineers. Aim of this chapter is not to give a vast description of Finite Element Method and its mathematical background but to summarize basic concept used in the simulation of electric machinery. Practical overview of finite element method applied to two dimensional problems is given in [1] and also in reference manual of Opera 2D software package [16] which will be used for all simulations described in this thesis.

The finite element method is essentially based on the subdivision of the whole domain in a fixed number of sub-domains. The advantage of subdividing the whole domain into a large number of small sub domains is that the problem becomes transformed from a small but difficult to solve problem into a big but relatively easy to solve problem. In each sub-domain the interpolating function is defined and the solution of the field problem is obtained when unknown coefficients of the interpolating function are calculated. For analysis of magnetic fields, it is convenient to use (and it is adopted in most of the FE software packages) formulation based on magnetic vector potential. The advantage of using the vector potential formulation is that all the conditions to be satisfied have been combined into a single equation. All other quantities, like flux density or field strength, may be easily derived from distribution of magnetic vector potential over the analyzed domain. The procedure of Finite Element Analysis contains these steps:

1. Division of the problem domain. The whole problem domain is subdivided in number of elements. The finesse of subdivision greatly affects accuracy of the solution. In general with larger number of smaller elements better accuracy can be achieved but it also influences the memory space required to the computer. In two-dimensional problems, the domain is a area and each sub-domain is a polygon, usually a triangle or a rectangle.
2. Choice of interpolating functions. Very simple functions are used for approximation of the unknown functions in elements because the sub-domains are usually small compared to the whole problem domain.
3. Formulation of the system of equations. Several standard methods are used for formulation, detailed description can be found in [1].
4. The Solution of the problem is obtained by solving the resulting system of equations. Value of the unknown function has to be computed in each node of the sub-divided domain.

All these steps are automated in available FE software packages and user doesn't have to know all details about the process, however, it is good to understand a main ideas and concepts.

Even though the three dimensional FE analysis can be used, the majority of the field problems concerning the analysis of electrical machines can be carried out by two-dimensional analysis [1]. This simplification greatly reduces computation time and brings several other advantages. Three dimensional effects that can't be neglected are usually taken into account by means of correction factors or analytical formulas. Good example is the end winding leakage reactance which has to be computed separately, by analytical equation, and then added to the result of the two-dimensional simulation by external electrical circuit coupled to the FE model.

All simulations in this thesis are considered with planar symmetry, which means that the analysis is carried out in the plane (x,y axis) perpendicular to the axial length of the machine (z axis). Following simplifications are assumed

- The Current density and the magnetic vector potential have only z component.
- The magnetic flux density and the magnetic field strength have x and y components.

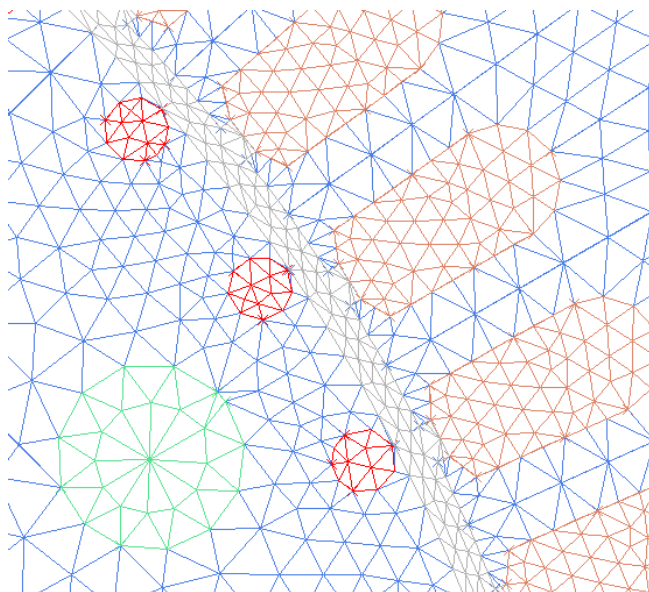


Fig. 13- Finite element mesh of two dimensional model of the synchronous generator

## 5.1 Boundary conditions

In the pre-processing stage of the simulation, the boundary conditions have to be assigned to get meaning full problem solution. Following section gives overview of basic boundary conditions used during the work on this thesis.

First is so called Dirichlet's Condition. It assumes that value of magnetic vector potential is known on a given part of the boundary. Generally, the value that is assigned is constant, so that the boundary line assumes the same value of magnetic vector potential. With this condition assigned, the flux lines are tangential to the boundary and no flux line crosses the boundary. Such a condition is equivalent to considering a material with zero magnetic permeability outside the analyzed domain. For simulation of a synchronous machine using planar symmetry, this condition is assigned to the external circumference of the stator. In reality this assumption is not true, but it simplifies the problem and gives sufficient accuracy.

Second condition is called Neumann's boundary condition. First derivative of the magnetic vector potential is assigned to the boundary forcing the flux lines to cross the boundary with a given angle. In case of homogenous condition, the flux lines are perpendicular to the boundary. Such a condition is equivalent to considering a material with infinite magnetic permeability outside the analyzed domain. With reference to the Fig.14, showing the cross section of analyzed machine, Homogenous Neumann's boundary condition may be assigned to the sides of the pole domain. However, more convenient is to use one of the periodic conditions.

Periodic boundary condition is useful in structures, that exhibit a repetition of the electromagnetic fields, but neither Dirichlet's nor Neumann's boundary condition is appropriate. Magnetic circuit of the synchronous machine consists of two or more poles with identical geometry and filed distribution. Assigning periodic condition along the pole sides may greatly reduce the analyzed domain thus only one fourth of the machine has to be modelled. This simplification reduces computation time and allows finer subdivision of the remaining part of the model.

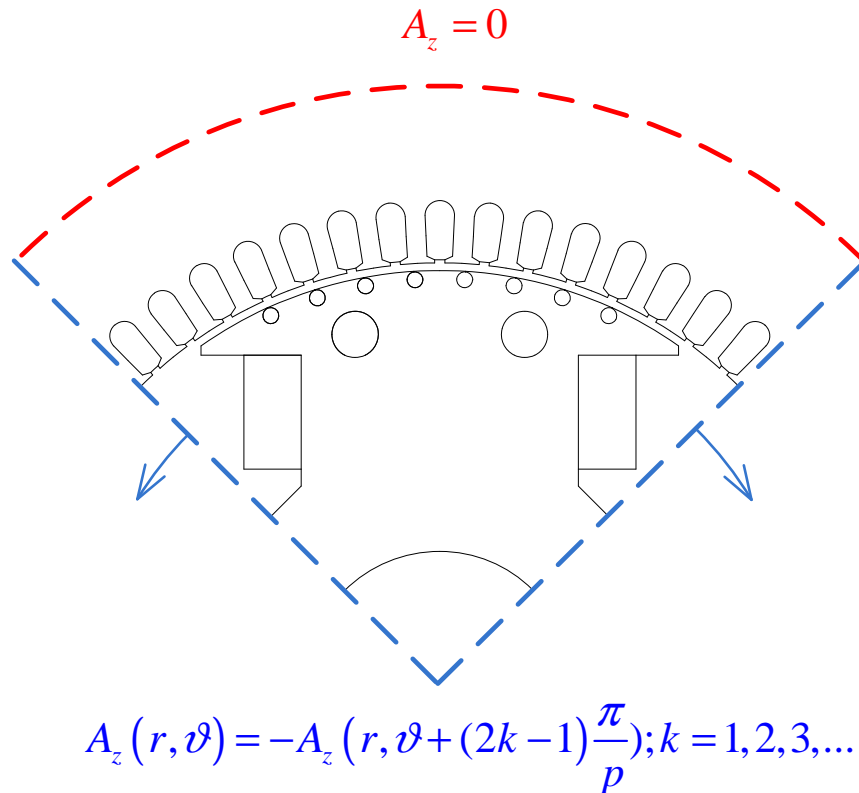


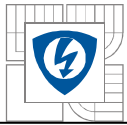
Fig. 14- Assignment of boundary conditions for simulation of synchronous machine

Once the geometry of the model is created and boundary conditions are identified and assigned to the model boundary lines, model is almost ready for solution. The excitation in magnetic model is done by assigning of current densities (either directly or by external circuit with voltage source and resistivity connected in series) to certain areas representing the cross section of conductors. The solution of the field problem consists of the knowledge of magnetic vector potential distribution across the analyzed domain.

## 5.2 Magnetostatic problems

Magneto-static problems are considered as zero or low frequency problems thus the fields are assumed to be time invariant. Obviously, synchronous machine is alternating current machine, but the relative speed of the rotor and armature reaction magnetic field is zero under steady state operation, therefore the analysis may be carried out using magneto-static solver. For time invariant magnetic field, following equations:

$$\begin{aligned} \nabla \times H &= J \\ \nabla \cdot B &= 0 \end{aligned} \quad (1.5)$$



For non-linear materials, such as magnetic steel of synchronous machine magnetic circuit, the permeability is defined as follows:

$$\mu = \frac{B}{H(B)} \quad (1.6)$$

Most of the FE packages use the magnetic field formulation by means of magnetic vector potential. With vector potential, magnetic flux density may be written:

$$B = \nabla \times A \quad (1.7)$$

Equation (1.7) may be rewritten, with respect to the equations (1.5) and (1.6), as follows:

$$\nabla \times \left( \frac{1}{\mu(B)} \nabla \times A \right) = J \quad (1.8)$$

Which is the equation solved in case of magneto-static problem with material permeability defined by non-linear characteristic.

### 5.3 Time harmonic problems

The time harmonic or steady state AC analysis solves eddy current problem where the driving currents or voltages are varying sinusoidally in time. This technique will be used for stand still frequency response test of analyzed generator. If the magnetic field is time varying, eddy currents can be induced in conductive materials and several other equations has to be added to static formulation.

Induced current density, in conductive bodies, is given by:

$$J = -\sigma A \quad (1.9)$$

After substitution in equation (1.8):

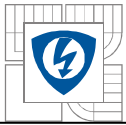
$$\nabla \times \left( \frac{1}{\mu(B)} \nabla \times A \right) = -\sigma A + J_{src} \quad (1.10)$$

Where  $J_{src}$  represents the applied current sources in the problem domain. Time harmonic solver solves the problem, where the field is oscillating at constant frequency thus equation (1.10) may be rewritten:

$$\nabla \times \left( \frac{1}{\mu(B)} \nabla \times a \right) = -j\omega\sigma a + J_{src} \quad (1.11)$$

Harmonic problems are usually modelled with constant permeability. However, modern FE packages allow the approximate calculation of saturation effects. During the quasi nonlinear simulation, element values are calculated from the maximum field in the AC cycle. Potential and current density can be expressed as real part of complex functions:

$$Ae^{j\omega t}, J e^{j\omega t} \quad (1.12)$$

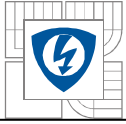


## 5.4 Transient problems

When the true time variations of machine quantities of the running synchronous generator are studied, the field has to be solved with a FEM *time stepping method*, in which the rotor is displaced at each time step by an angle corresponding to the angular velocity of the rotor. The field equation is given by:

$$\nabla \times \left( \frac{1}{\mu(B)} \nabla \times A \right) = J_{src} - \sigma \frac{\partial A}{\partial t} \quad (1.13)$$

Current density is split into two components. First component is current induced in conductive bodies and the second is the source current density. Transient problems are analyzed using Rotating Machine solver, where FE model is coupled with external electrical circuit thus source current density is computed from applied voltage and external circuit parameters. Also three dimensional effects, such as end winding leakage, area taken into account by an external reactance connected in series to the voltage source.



## 6 IDENTIFICATION OF SYNCHRONOUS REACTANCE

Procedure of synchronous reactance calculation from FE field solution is well known and widely described in literature. Magnetostatic simulation is performed and then the flux linkage is computed from field solution.

### 6.1 Analytical expression of synchronous reactance

Main armature reaction inductance of electrical machine is defined by dimensions of magnetic circuit, winding distribution and properties of used materials. In this section the main magnetizing inductance for poly-phase, non-saturated machine is derived.

Derivation is simplified by assumption that the distribution of magnetic flux density on the rotor surface is sinusoidal over a pole pitch  $\tau_p$  and there is no variation with respect to the machine equivalent axial length  $l'$ . The peak value of air gap magnetic flux linkage is integral of flux density over a pole face area  $A$ , multiplied by number of effective single phase stator winding turns.

$$\Psi_m = (k_{ws1} N_s) \int_A B dA = k_{ws1} N_s \frac{2}{\pi} \tau_p l' B_m \quad (1.14)$$

Where  $N_s$  is number of turns of single phase stator winding and  $k_{ws1}$  is a winding factor. For full pitched lap winding, the winding factor is:

$$k_{ws1} = \frac{\sin \frac{\pi}{6}}{q \sin \frac{q\pi}{6}} \quad (1.15)$$

Where  $q$  is a number of slots per pole and per phase. Flux density in the air gap is given by:

$$B_m = \frac{\mu_0}{g''} F_m = \frac{4}{\pi} \frac{\mu_0 k_{ws1} N_s}{2 p g''} \sqrt{2} I_s \quad (1.16)$$

Where  $g''$  is equivalent air gap and  $F_m$  is magneto motive force of single phase stator winding. After substitution of (2.5) in equation (2.1) we may obtain flux linkage of a single phase.

$$\Psi_m = \frac{4 \mu_0 \tau_p l' (k_{ws1} N_s)^2}{\pi^2 p g''} \sqrt{2} I_s \quad (1.17)$$

Main armature reaction inductance for  $m$ -phase non-salient machine is given by division of magnetic flux linkage and magnetizing current according to equation 2.7.

$$L_m = \frac{m}{2} \frac{\Psi_m}{I_m} = \frac{m}{2} \frac{\Psi_m}{\sqrt{2} I_s} = \frac{m}{2} \frac{2 \mu_0 \tau_p l' (k_{ws1} N_s)^2}{\pi^2 p g''} = \frac{m \mu_0 l' D_g}{\pi p^2 g''} (k_{ws1} N_s)^2 \quad (1.18)$$

It appears from the above equation that value of armature reaction inductance depends on stator bore diameter  $D_g$ , number of phases  $m$ , number of pole pairs  $p$ , effective number of stator winding turns, effective length of air gap  $g''$  and equivalent axial length of magnetic circuit  $l'$ .



Equivalent axial length incorporates influence of magnetic field fringing at the edges of magnetic circuit and is approximately given by:

$$l' \approx l + 2g_0 \quad (1.19)$$

The equation 3.4 is suitable for all types of salient synchronous machines because the impact of various rotor geometries is incorporated in the value of equivalent air gap. In case of salient machine, such as the analyzed machine, the difference between d and q-axis inductance is expressed by a different value of effective air gap for each axis.

$$L_d = \frac{3\mu_0 l' D_{gd}}{\pi p^2 g_d''} (k_{ws1} N_s)^2$$
$$L_q = \frac{3\mu_0 l' D_{gq}}{\pi p^2 g_q''} (k_{ws1} N_s)^2 \quad (1.20)$$

Equivalent air gap is value of physical air gap of the machine, multiplied by lengthening factors. Equivalent air gap summarizes additional reluctances of the flux path into one value, equivalent to the actual magnetic circuit with smaller air gap. For instance, slotting of the stator bore is taken into account by so-called Carters factor. Slotted stator is then replaced by smooth but with longer, equivalent. Air gap. For salient pole machine, the q axis equivalent air gap is usually three times longer than in d axis.

## 6.2 Calculation of flux linkage from field solution

First step in calculation of synchronous reactance is calculation of flux linked with stator winding. Stator winding inductance is then calculated as a ratio of flux linkage and current. [X] describes two methods of flux linkage estimation:

1. Flux linkage calculated from magnetic vector potential:

Flux linkage is calculated as a product of the number of turns, axial length of magnetic circuit (length in z-axis) and the difference in the vector potential at the location of the two coil sides.

2. Flux linkage calculated from air gap flux density:

In general flux through the oriented surface is calculated by surface integral of magnetic flux density. In case of the two dimensional problem, the flux is computed by line integral of magnetic flux density along the oriented line and result is multiplied by depth of the problem. Integral along circular line between rotor and stator is performed for calculation of flux linkage in a radial flux machine, such as analyzed synchronous generator.

Only first method will be described in detail and considered in further analysis because second method doesn't take into account slot leakage and this has to be calculated separately. Using the Stokes theorem, magnetic flux can be computed as the loop integral of the magnetic vector potential along the closed line bordering the surface. Flux is then given by:

$$\phi = \int_S \mathbf{B} \cdot \mathbf{n} \cdot d\mathbf{S} = \oint_l \mathbf{A} \cdot d\mathbf{l} \quad (1.21)$$

Integration line on the fig.X represents the coil of the machine. Problem is modelled using planar symmetry thus magnetic vector potential has only z-axis component which is



assumed to be constant along the z axis. The magnetic flux, linked with the coil, is equal to the difference of z axis component of the magnetic vector potential in two coil sides times the depth of the problem.

$$\phi = (A_{z1} - A_{z2}) \cdot L \quad (1.22)$$

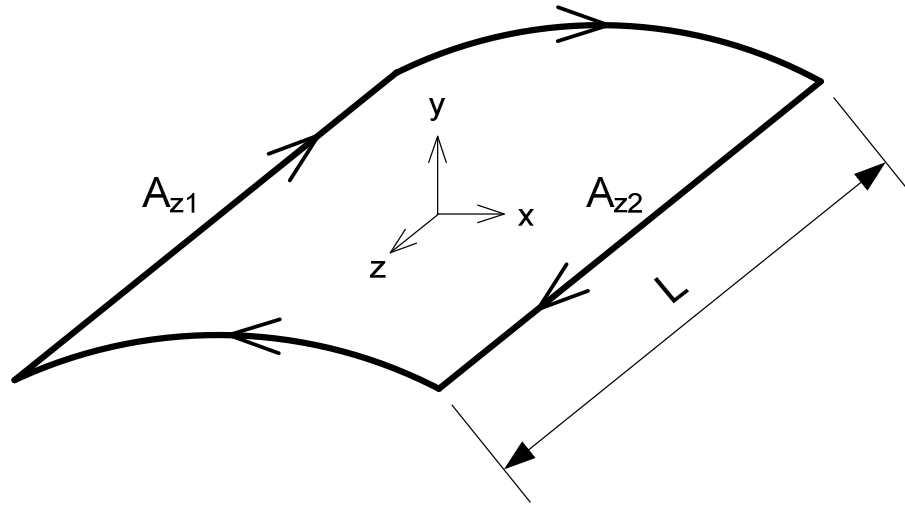


Fig. 15- Integration path for calculation of flux linkage from magnetic vector potential

In the case of real conductors it is convenient to consider average value of  $A_z$  across the slot cross section and this may be calculated as follows.

$$A_z = \frac{1}{S_q} \int_S A_z dS \quad (1.23)$$

Where  $A_z$  is z-axis component of magnetic vector potential and  $S_q$  is slot cross section. Referring to the FE model showed in chapter five, the flux linkage of the j-th phase winding is calculated by following equation.

$$\psi_j = 2pL_{Fe} \frac{n_q}{n_{pp}} \sum_{q=1}^{Q/2p} k_{jq} \frac{1}{S_q} \int_{S_q} A_z dS \quad (1.24)$$

Where  $2p$  is number of pole pairs,  $L_{Fe}$  is axial length of magnetic circuit,  $Q$  is number of slots,  $n_q$  is number of conductors in each slot,  $n_{pp}$  is number of parallel paths of the machine and  $k_{jq}$  is coefficient taking into account whether the conductors in the q-th slot are of the j-th phase or not, as well as the conductor orientation. Analyzed machine has double layer winding thus coefficient  $k_{jq}$  assumes the following values:

- $k_{jq}=0$  if the conductors in the q-th slot doesn't belong to the j-th phase
- $k_{jq}=\pm 1$  if both conductors in the q-th slot belongs to the j-th phase.
- $k_{jq}=\pm 0.5$  if only one conductor in the q-th slot belongs to the j-th phase.

Plus or minus sign represents orientation of the conductor with respect to the z-axis direction.

## 6.3 Open circuit characteristic

The open circuit characteristic of synchronous machine is a curve of the open circuit armature terminal voltage as a function of field current when the machine is driven by prime mover at synchronous speed. This characteristic represents the relation between fundamental component of air gap flux and magneto motive force acting on the magnetic flux path when the field winding is the only source of MMF.

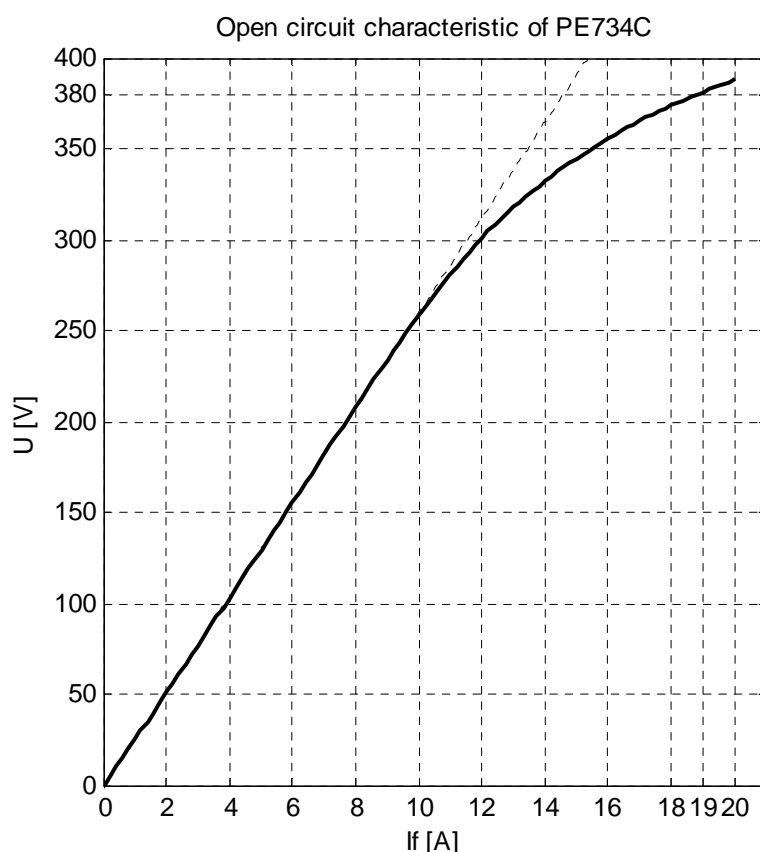


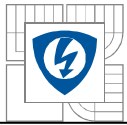
Fig. 16- Output line to line voltage as a function of field current

In general there are two ways how to mimic the actual test procedure. First option is to use time stepping solver. Rotor is magnetized by field current and revolves at constant synchronous speed. As a result of this EMF is induced across the open circuited armature winding. Value of emf is calculated for each time step of the simulation therefore full open circuit voltage waveform is obtained.

Second option employs magneto static solver and is based on well known relationship between induced EMF and magnetic flux linkage. Rotor is aligned so that the maximum flux, produced by excited field winding, is linked with a-phase coil and this flux is computed from the magnetic vector potential or air gap flux density. RMS value of open circuit voltage is then given by

$$V_a = \frac{1}{\sqrt{2}} \omega \psi_a \quad (1.25)$$

From figure () impact of magnetic saturation can be clearly seen. Open-circuit characteristic is initially a linear function but with increasing field current tends to bend downward because the saturation of the magnetic circuit increases the reluctance of main



flux path. Linear extension of the initial linear part of the characteristic is known as air-gap line and it represents unsaturated operation of the machine. Difference between air-gap line and the actual characteristic shows level of saturation of the magnetic circuit.

Characteristic also shows how much current has to be supplied to the field winding in order to produce rated voltage at the machine terminals and this information will be particularly useful for simulation of sudden short circuit.

## 6.4 Calculation of $X_d$

The synchronous direct axis reactance may be defined as the reactance of that phase winding whose axis coincides with the direct axis of the rotor, when the three-phase currents are flowing through the armature windings. Magneto static solver may be used for the calculation because relative speed of the rotor and the armature reaction field is zero.

Simulation is simplified by means of geometrical symmetry of the machine, thus only one pole is modelled and boundary conditions are assigned according to figure(). Field current is assumed to be zero so that magnetic field is excited only by armature currents. The phase currents in balanced three phase system are given by:

$$\begin{aligned}i_a(t) &= I_{\max} \sin(\omega t) \\i_b(t) &= I_{\max} \sin\left(\omega t - \frac{2\pi}{3}\right) \\i_c(t) &= I_{\max} \sin\left(\omega t + \frac{2\pi}{3}\right)\end{aligned}\quad (1.26)$$

Where  $I_{\max}$  is a peak value of phase current,  $\omega$  is angular velocity. In magneto static simulation DC currents are injected in conductors, thus time instant  $t$  has to be chosen in order to get maximum of the MMF distribution coinciding with direct axis. With winding distribution of figure() this time instant equals zero. Injected DC currents are then given by:

$$\begin{aligned}i_a &= I_{\max} \\i_b &= -\frac{I_{\max}}{2} \\i_c &= -\frac{I_{\max}}{2}\end{aligned}\quad (1.27)$$

After the field solution is obtained flux linkage is computed by means of magnetic vector potential. In general, direct axis inductance is given by following formula:

$$L_d = \frac{\psi_d}{I_d} \quad (1.28)$$

Figure shows that a-phase axis coincides with the direct axis, therefore direct axis reactance can be computed as follows:

$$X_d = \omega \frac{\psi_d}{I_d} = \omega \frac{\psi_a}{I_a} = \omega \frac{\psi_a}{I_{\max}} \quad (1.29)$$

Simulation was carried out without field winding excited. It is possible to do the simulation even with field winding magnetized, but the value of filed flux has to be computed and then subtracted from total flux linkage of the d axis coil in order to get the d axis reactance as a ratio of d axis flux linkage to d axis current. This assumption may be adopted only in case of linear simulation, where simple superposition of total flux takes place.

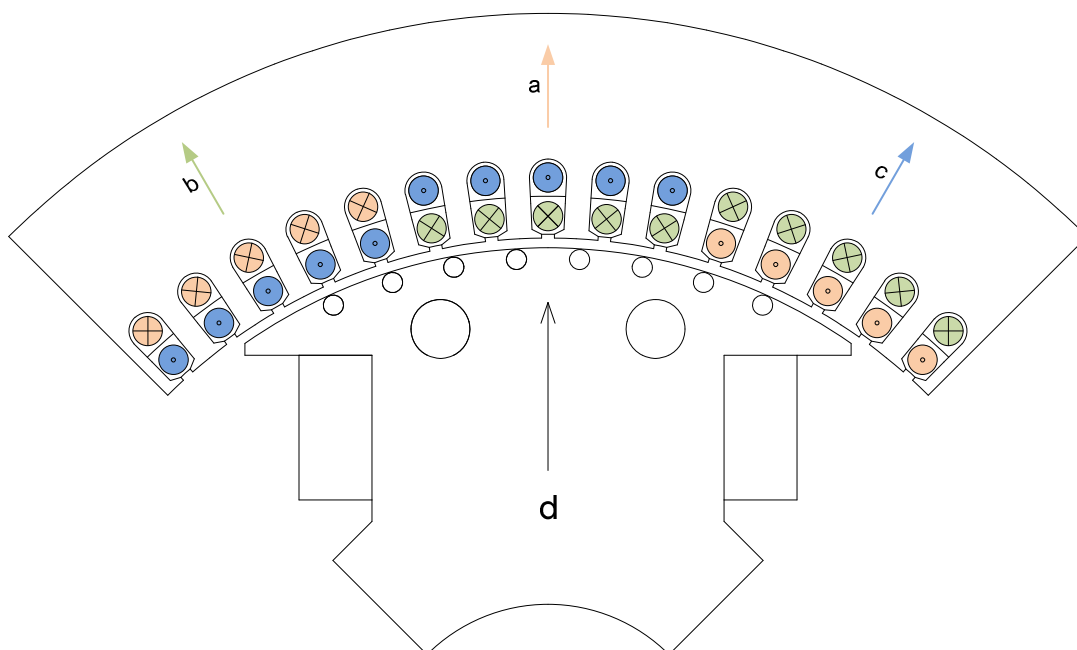


Fig. 17- Winding configuration for calculation of d axis reactance

Due to the nonlinear properties of steel laminations the value of reactance is affected by saturation of magnetic circuit, therefore the calculation has to be repeated for several values of d axis current in order to capture the reactance profile.

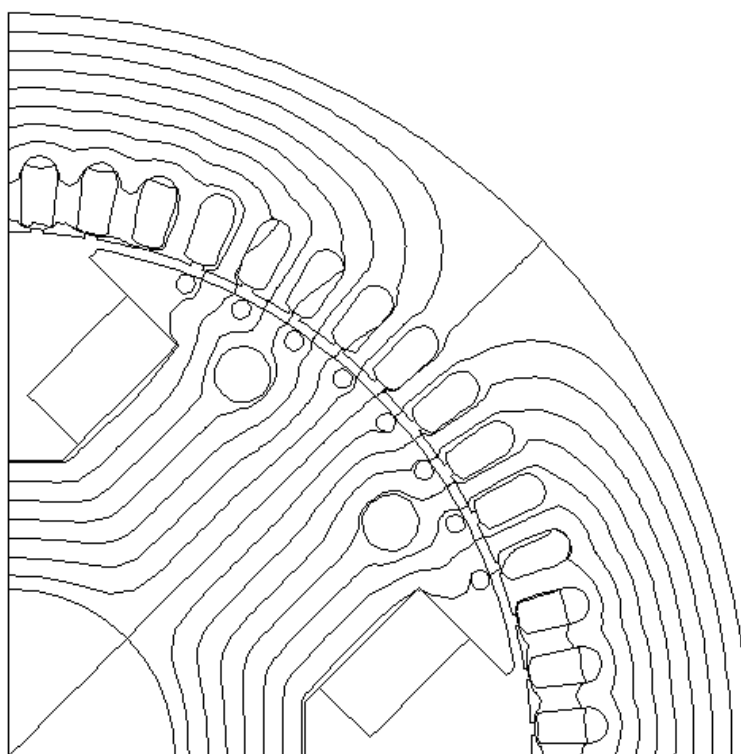


Fig. 18- Flux plot for armature winding excited by pure d axis current

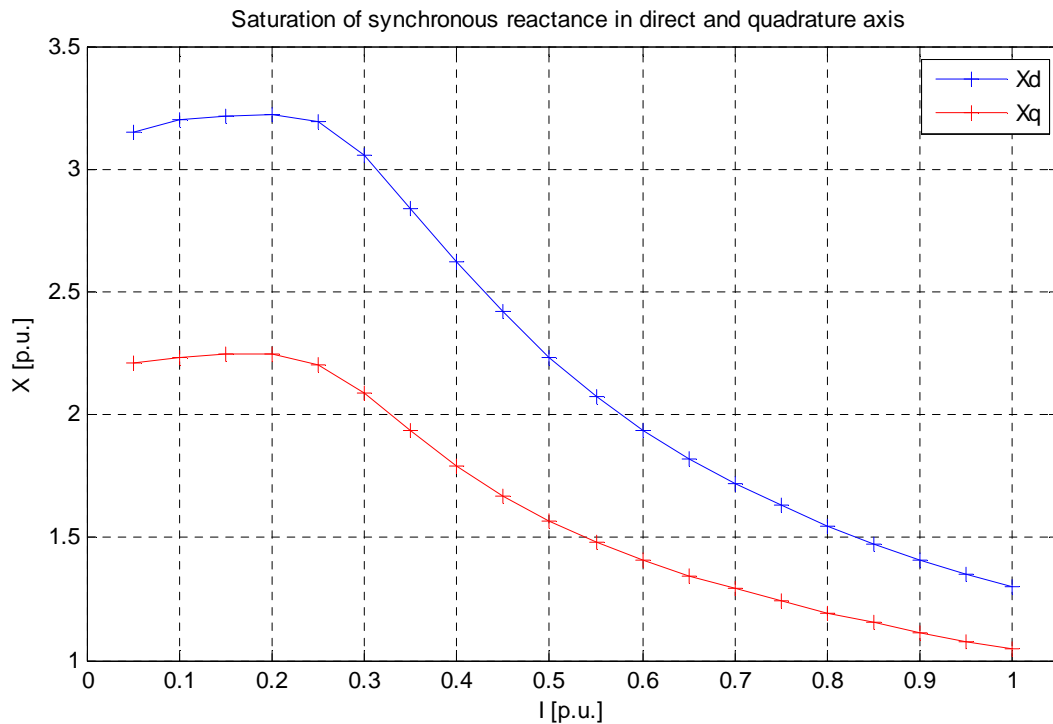


Fig. 19- Impact of saturation on the values of synchronous reactance

## 6.5 Calculation of $X_q$

The calculation of q axis reactance is carried out the same way as for the direct axis, only difference is that in this case the maximum value of the MMF distribution is aligned with quadrature axis.

$$X_q = \omega \frac{\psi_q}{I_q} = \omega \frac{\psi_a}{I_{\max}} \quad (1.30)$$

Calculated results are given in per unit values because per unit system is often used in analysis of electric machinery and power systems. In general, the per unit values is the ratio of the actual value and the base value of the same quantity. Base values for analyzed machine are:

$$\begin{aligned} S_{base} &= 1404 \text{ kVA} \\ V_{base} &= 380 \text{ V} \\ X_{base} &= \frac{V_{base}^2}{S_{base}} = 0.103 \Omega \end{aligned} \quad (1.31)$$

Value of computed reactance in per unit system is then given by:

$$X_{p.u.} = \frac{X_{actual}}{X_{base}} \quad (1.32)$$

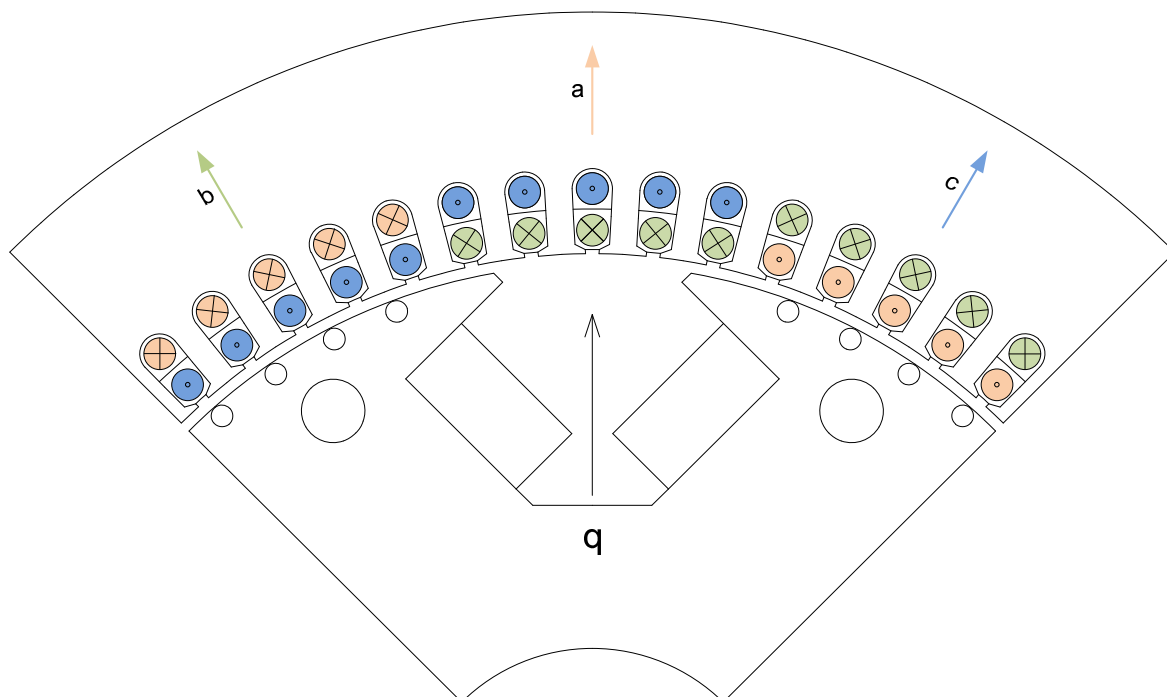


Fig. 20- Winding configuration for calculation of d axis reactance

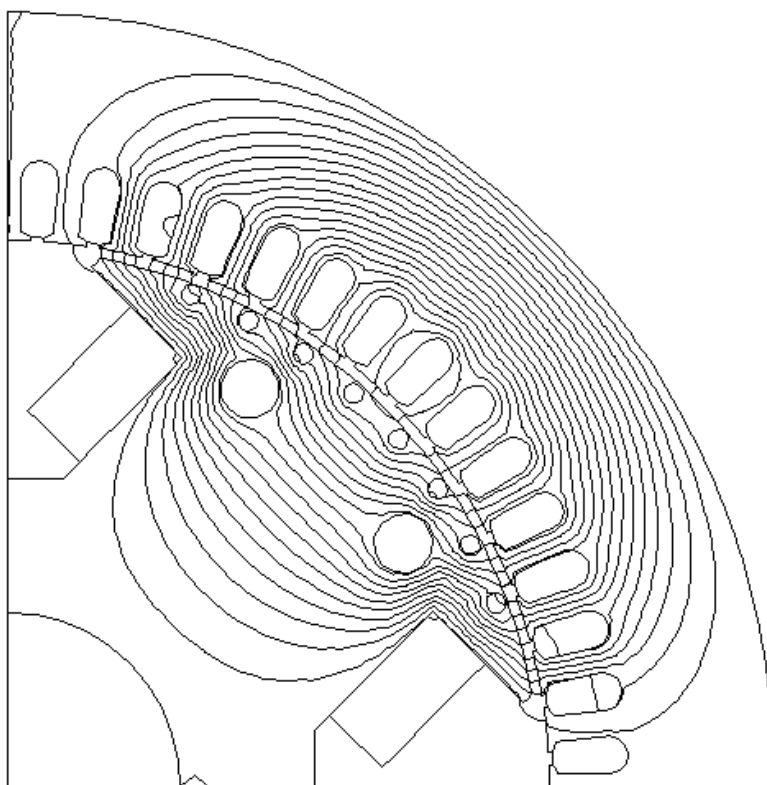
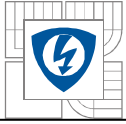


Fig. 21- Flux plot for armature winding excited by pure q axis current



## 6.6 Impact of cross coupling

The cross coupling can be defined as a magnetic interaction between direct and quadrature axis []. This section is focused on investigation of this phenomenon and its impact on synchronous reactance.

Simulation performed in previous chapter assumes non-linear magnetic circuit but doesn't take into account cross saturation. Flux linkages are then given by

$$\psi_d(i_d) = L_d(i_d) \cdot i_d + \psi_{dm}; \psi_q(i_q) = L_q(i_q) \cdot i_q \quad (1.33)$$

Where direct and quadrature axis synchronous inductance is a function of imposed current in its axis. With high level of saturation flux path in d axis may become saturated by q axis flux and vice versa. For this case equation () may be rewritten as follows.

$$\psi_d(i_d, i_q) = L_d(i_d, i_q) \cdot i_d + \psi_{dm}; \psi_q(i_q, i_d) = L_q(i_q, i_d) \cdot i_q \quad (1.34)$$

Synchronous reactance is then two-dimensional function of currents in both axis. Simulation procedure is straightforward and it can be done using the same model as in previous cases.

1. Stator current in each phase is calculated from d and q axis current components using inverse park transformation. These currents are then injected into stator slots according to winding distribution diagram.

$$\begin{bmatrix} I_a \\ I_b \\ I_c \end{bmatrix} = \begin{bmatrix} \cos(\vartheta_m) & \sin(\vartheta_m) \\ \cos(\vartheta_m + \frac{2\pi}{3}) & -\sin(\vartheta_m + \frac{2\pi}{3}) \\ \cos(\vartheta_m + \frac{2\pi}{3}) & -\sin(\vartheta_m + \frac{2\pi}{3}) \end{bmatrix} \cdot \begin{bmatrix} I_d \\ I_q \end{bmatrix} \quad (1.35)$$

2. Flux linkage of each phase coil is computed from magnetic vector potential and then is transformed into reference frame by means of park transformation.

$$\begin{bmatrix} \psi_d \\ \psi_q \end{bmatrix} = \frac{2}{3} \begin{bmatrix} \cos(\vartheta_m) & \cos(\vartheta_m - \frac{2\pi}{3}) & \cos(\vartheta_m + \frac{2\pi}{3}) \\ -\sin(\vartheta_m) & -\sin(\vartheta_m - \frac{2\pi}{3}) & -\sin(\vartheta_m + \frac{2\pi}{3}) \end{bmatrix} \cdot \begin{bmatrix} \psi_a \\ \psi_b \\ \psi_c \end{bmatrix} \quad (1.36)$$

3. D and q axis reactance is calculated from d and q axis flux linkage component and known value of current in each axis.

$$X_d = \omega \frac{\psi_d}{I_d}; X_q = \omega \frac{\psi_q}{I_q} \quad (1.37)$$

4. Because reactance in each axis is in this case two-dimensional function of d and q axis current it may be plotted as a contour diagram.

Reactances obtained in this way may be adopted in complex dynamic models in a form of look up table, where input is current components and output is a value of reactance.

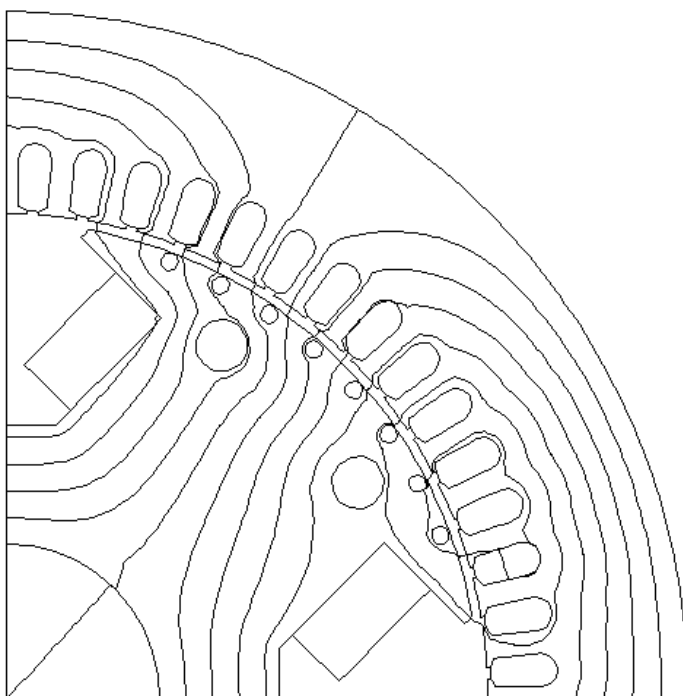


Fig. 22- Flux plot for armature winding excited by armature current with d and q axis komponent

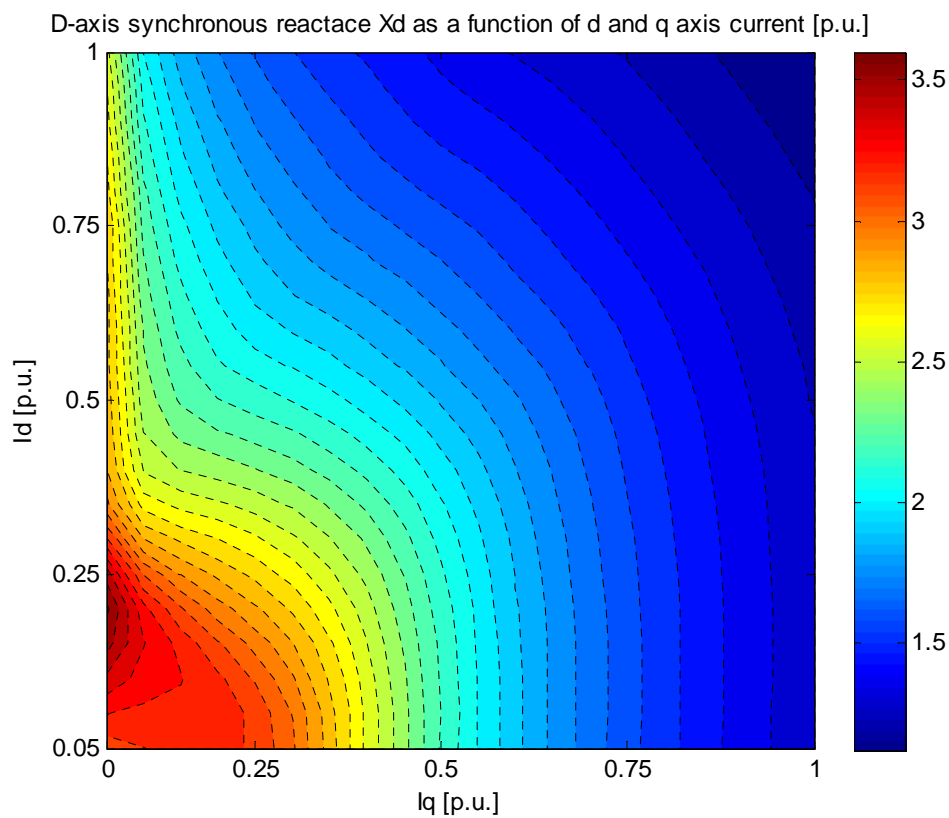


Fig. 23- D axis synchronous reactance as a function of d and q axis current in a form of contour plot



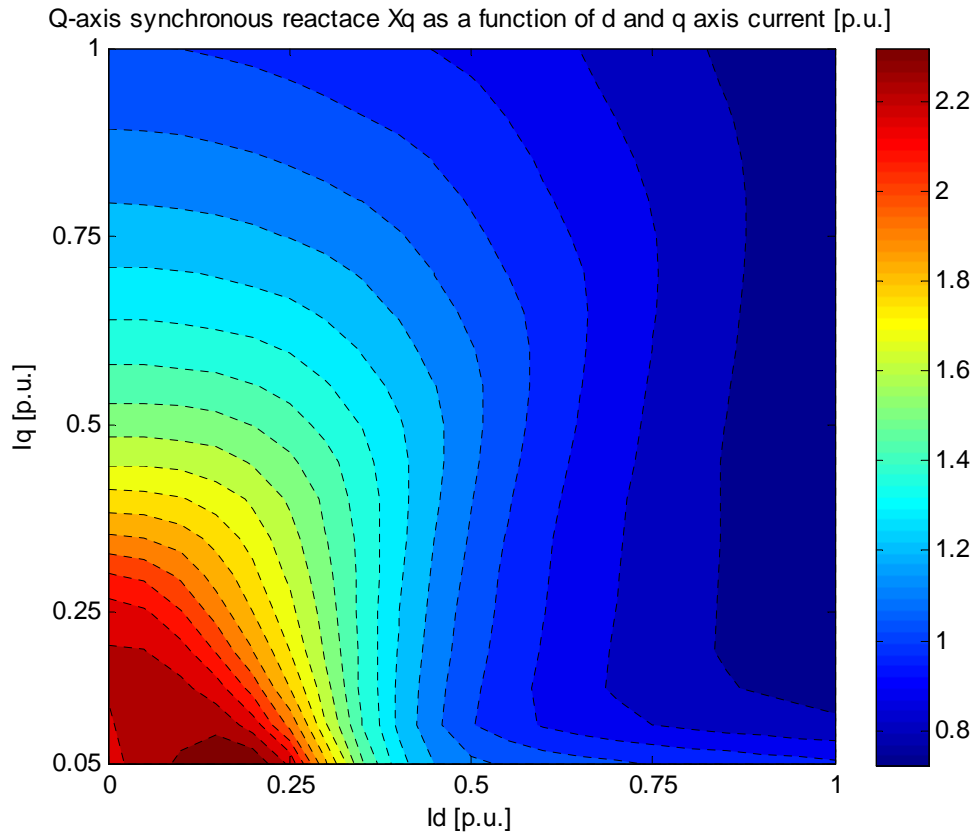


Fig. 24- Q axis synchronous reactance as a function of d and q axis current in a form of contour plot

## 6.7 Calculation of end winding leakage reactance

Above mentioned simulations neglects three dimensional effects such as fringing of the magnetic field at the ends of the magnetic circuit and the impact of end winding leakage. There are two options how to add these effects to results of two-dimensional analysis. First option is to create three-dimensional model of the winding overhangs and then perform FE simulation. Reactance is then obtained by post processing of the field solution. More common approach is to use analytical expression based on calculation of effective end winding length and permeance coefficients. Second method will be considered even though it might produce larger error.

$$X_{ew} = \omega \frac{4m}{Q} q N^2 \mu_0 l_w \lambda_w \quad (1.38)$$

Where  $m$  is number of phases,  $Q$  is number of stator slots,  $q$  is number of slots per pole and phase,  $N$  is number of turns in series,  $l_w$  is effective length of end winding and  $\lambda_w$  is permeance factor. Product of the effective length and the permeance factor can be written as follows.

$$l_w \lambda_w = 2l_{ew} \lambda_{ew} + W_{ew} \lambda_w \quad (1.39)$$

Finally the value of permeance factors has to be obtained. The permeance factors depend on configuration of winding overhangs, end-winding dimensions and rotor saliency. Table of typical permeance factors for most common machines is given in [4].

## 7 IDENTIFICATION OF TRANSIENT AND SUBTRANSIENT REACTANCE

Definition of transient and subtransient reactance is not as clear as in case of synchronous one but these definitions are usually employed:

- The transient reactances of the synchronous machine are defined as the reactances associated with the armature reaction when a three phase positive sequence source is suddenly applied at the generator terminals, immediately after the short-lived subtransient phenomenon in the damper winding and rotor forging has subsided. The field winding is supposed to be short-circuited with the rotor spinning at the rated speed prior to the application of the source at the generator terminals. Depending on position of the armature fundamental mmf space waveform with respect to the pole axis, the transient direct and quadrature axis reactances are then distinguished.[10]
- The subtransient reactances of a synchronous machine are defined as the reactances associated with the armature reaction, immediately after a three phase positive sequence source is applied to the machine terminals with the rotor spinning at the rated speed and the field winding short circuited.[10]

Four different methods will be investigated, in this chapter, in order to simulate conditions according to the above mentioned definitions.

### 7.1 Magnetostatic calculation with modified boundary conditions

This method was introduced in [10] and it employs equivalent magneto static model in which the unknown sources of the induction nature are replaced by equivalent boundary condition. Because the magneto static solver is used, the computation time is short and post-processing is similar to calculation of synchronous reactance.

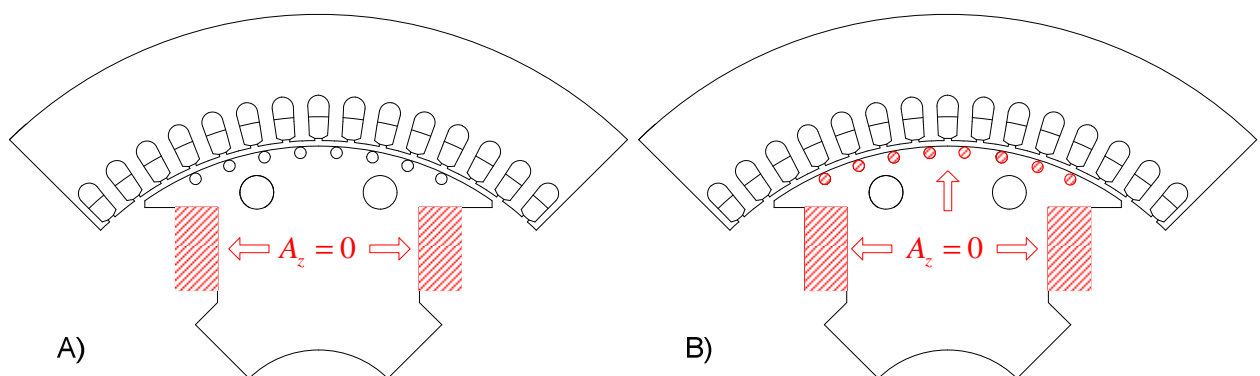


Fig. 25- Regions excluded from the FE model for A)transient conditions,B)subtransient conditions

Firstly the simulation is set up for calculation of transient conditions. The stator conductors are loaded in order to get maximum of MMF distribution aligned with corresponding axis of the rotor. For transient conditions the induced currents in damper winding are assumed to be zero but unknown induced currents exist in the field winding and they prevent armature flux from linking the field winding. In order to simulate this situation

the current carrying area of field winding is excluded from the simulated domain and it is replaced by equivalent boundary condition. It is assumed that the normal component of magnetic field at the surface of conductor vanishes establishing the equipotential. Dirichlet's boundary condition is imposed on boundaries of field winding region to represent the flux free zone.

The set up for simulation of subtransient conditions employs same principles, but in this case the damper winding regions are also excluded from the domain because unknown currents are induced in them during subtransient operation of the machine.

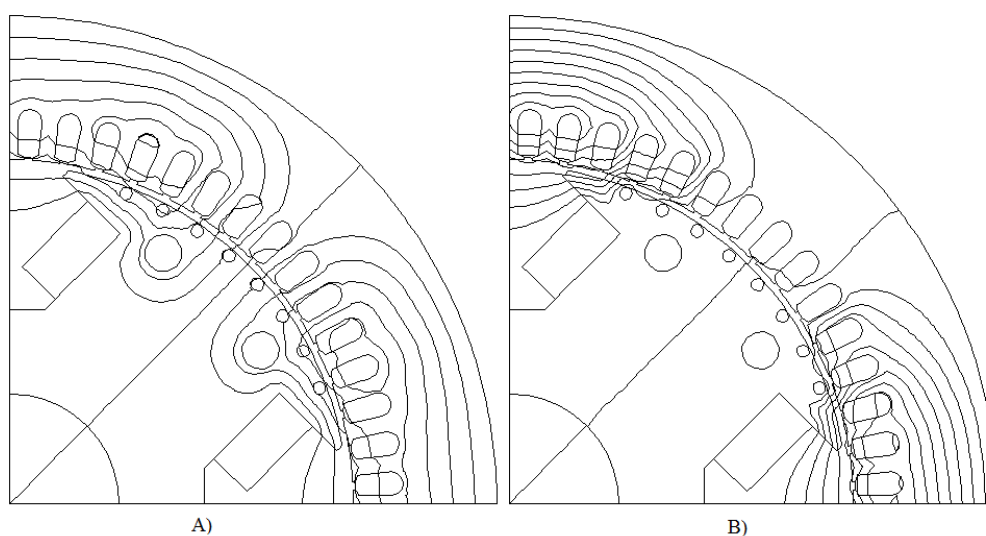


Fig. 26- Flux plots for model with modified boundary conditions. A) transient condition, B) sub-transient conditions

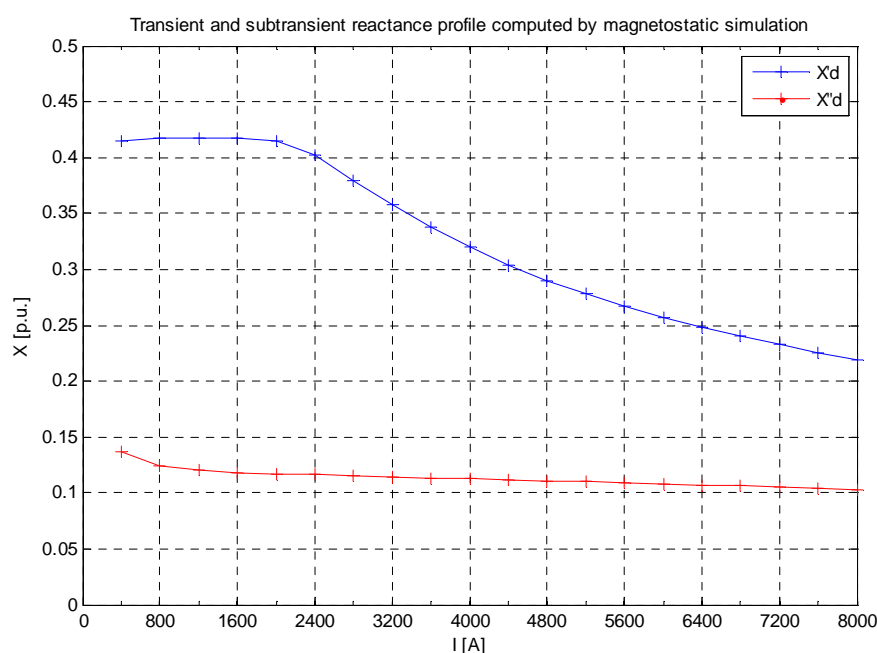


Fig. 27- Transient and subtransient reactance profile computed by magnetostatic simulation with modified boundary conditions

## 7.2 Time harmonic simulation

The second option how to simulate transient and subtransient conditions is the time harmonic simulation. Rotor of the machine is locked, with field winding short circuited, and armature winding is excited by current as in case of synchronous reactance calculation, only difference is that the current has a constant frequency. Transient and subtransient regime of the generator is distinguished by the value of imposed frequency. This method is described in [2] and was adopted in several papers, namely [12] and [13]. Flux linkage is obtained the same way as in case of synchronous reactance, but now it is a complex number.

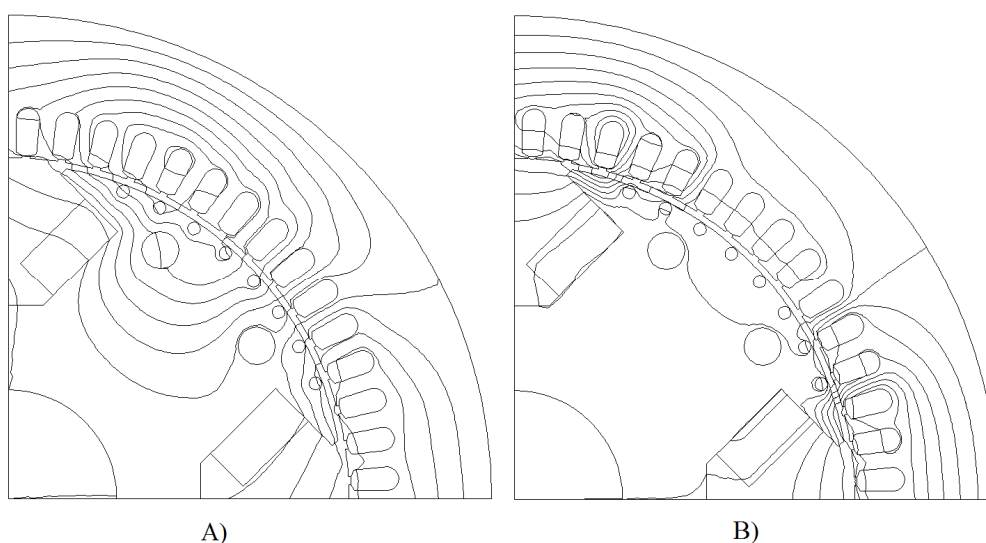


Fig. 28- Flux plots for Time harmonic simulation for different frequency of injected current A) transient condition  $f = 1\text{ Hz}$  B) subtransient condition  $f = 50\text{ Hz}$

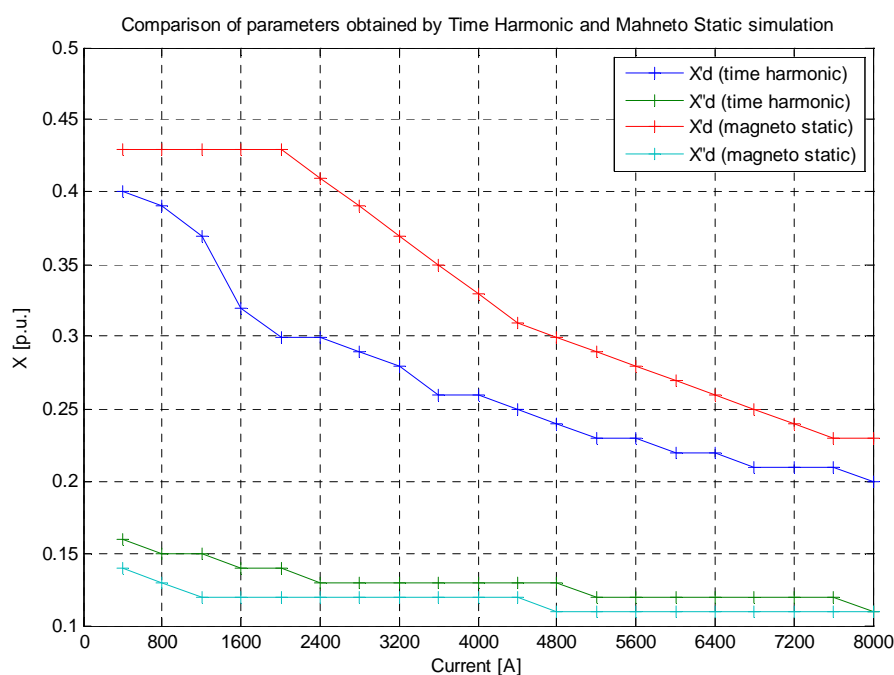


Fig. 29- Comparison of direct axis reactances obtained by magneto static simulation and by time harmonic simulation

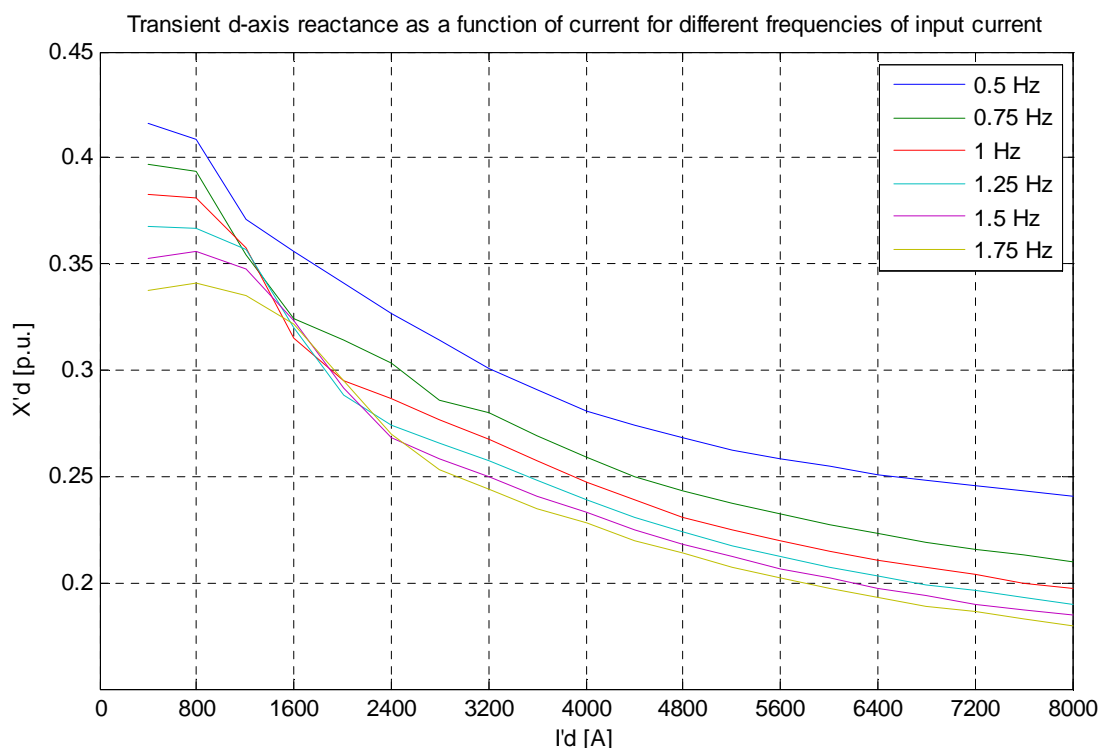


Fig. 30- Dependence of transient reactance profile on frequency of input current

### 7.3 Single frequency response simulation

Single frequency response simulation is the standard test method for measurement of d and q axis subtransient. Rotor is at stand still and it is aligned with direct or quadrature axis. Two armature winding phases are connected in series and supplied from voltage source of constant, nominal, frequency. Input voltage and current is measured. Schematic diagram of the method is given on Fig.31. Impedance is given by:

$$Z''_{d,q} = \frac{V}{2I} \Rightarrow X''_{d,q} = \sqrt{Z''_{d,q}^2 - R_s^2} \quad (1.40)$$

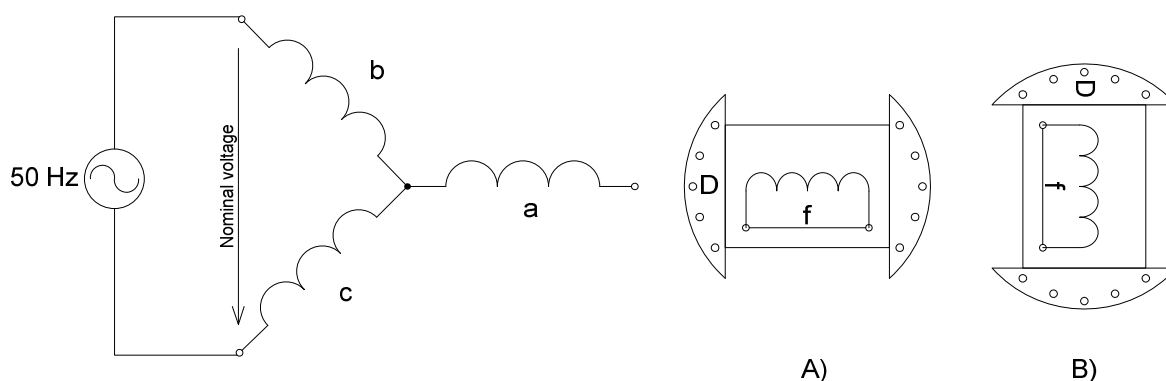


Fig. 31- Setup for Single Frequency Response Test for: A) d axis subtransient reactance  
B) q axis subtransient reactance

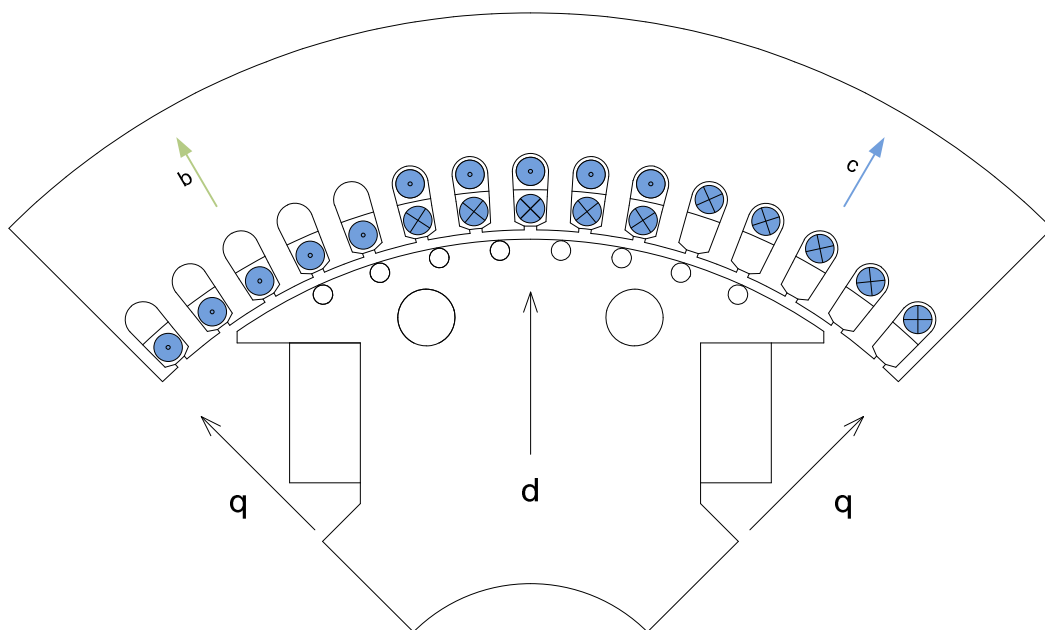


Fig. 32- Winding distribution for simulation of Single frequency response. Rotor is aligned with nominal frequency a-phase and coils of b and c phase are in series and connected to source of AC voltage

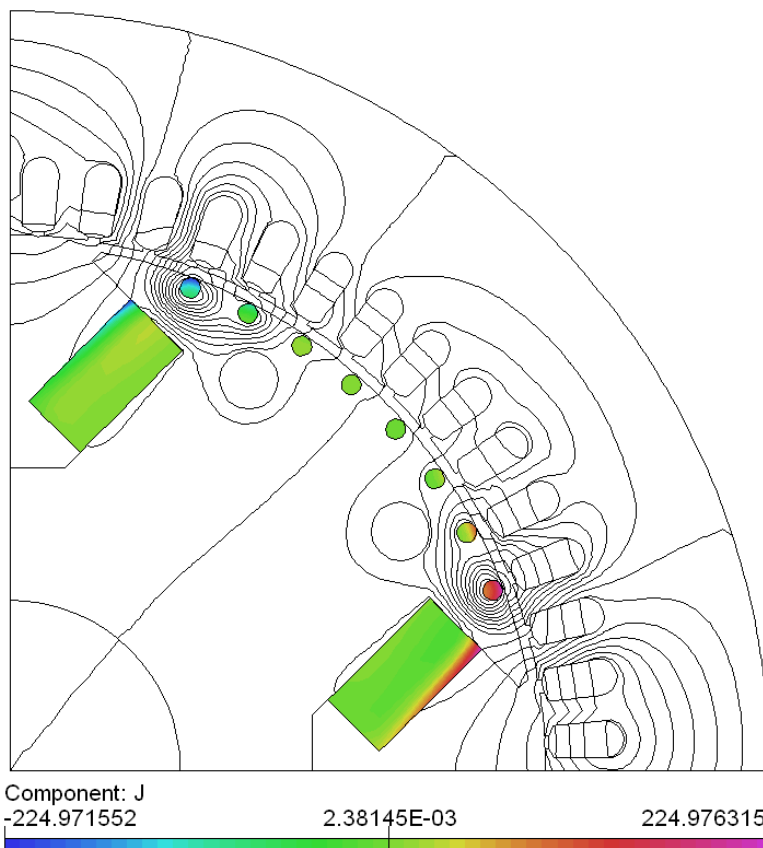


Fig. 33- Flux plot for Single Frequency Response simulation in direct axis, contours show the induced current density in damper and field winding

## 7.4 Sudden short circuit simulation

Purpose of this section is to carry out a non-linear time stepped FE simulation of a symmetrical three phase short circuit at synchronous machine terminals. As in case of Single Frequency Response simulation, this method mimics standard test procedure used in determination of synchronous machine parameters.

The Time-stepping solver is used, for purpose of simulation, coupled with external circuit. Procedure may be described by following points:

- Stator winding is defined by external circuit with inductance and resistivity connected in series. Resistance represents phase resistance of armature winding and the value of inductance is associated with leakage inductance of the armature winding overhangs.
- Rotor rotates at nominal speed during the whole simulation.
- Field winding is also represented by external circuit, with a field winding resistance and voltage source. Value of field voltage has to be set in order to get field current which will produce rated no-load voltage at machine terminals. Field voltage is constant during the short circuit simulation, but additional currents may be induced during transient operation.
- Short circuit is applied using parametric resistivity of armature winding. For initial no-load run the resistivity is large, thus very small current is flowing in the armature winding. At the chosen time instant, resistivity is switched to the value of phase resistance by external command file.
- Short circuit current traces are recorded up to the point when they reach sustained value.

Detailed description of post-processing of current traces is given in chapter devoted to testing of synchronous machine.

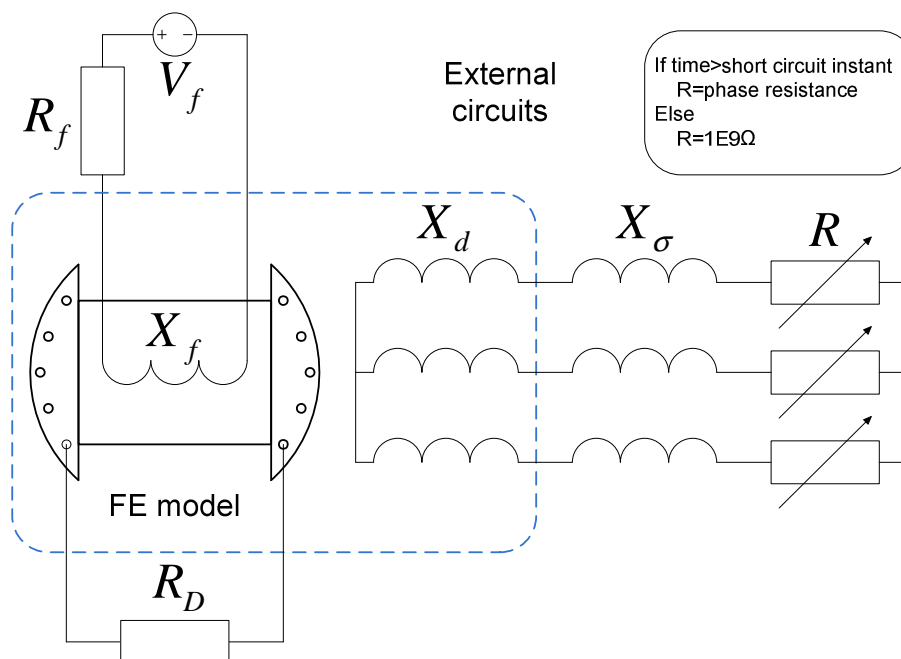


Fig. 34- FE model of synchronous machine coupled with external electrical circuits for short circuit simulation

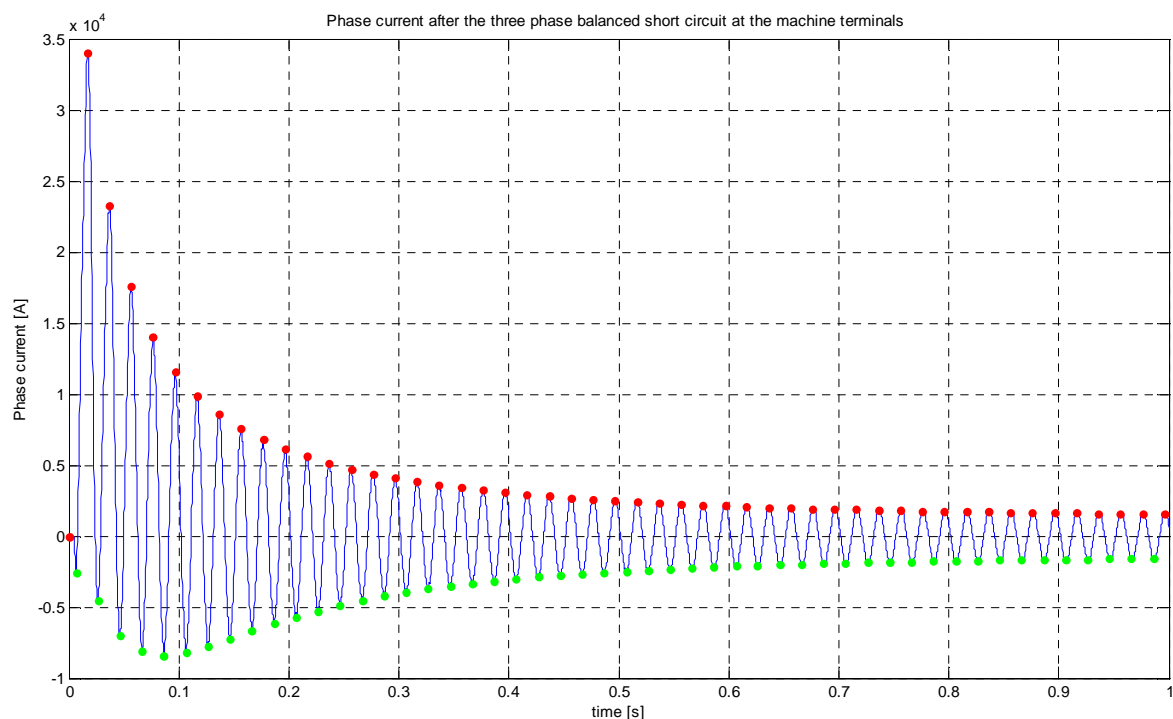


Fig. 35- Short circuit current trace with high-lighted peak values

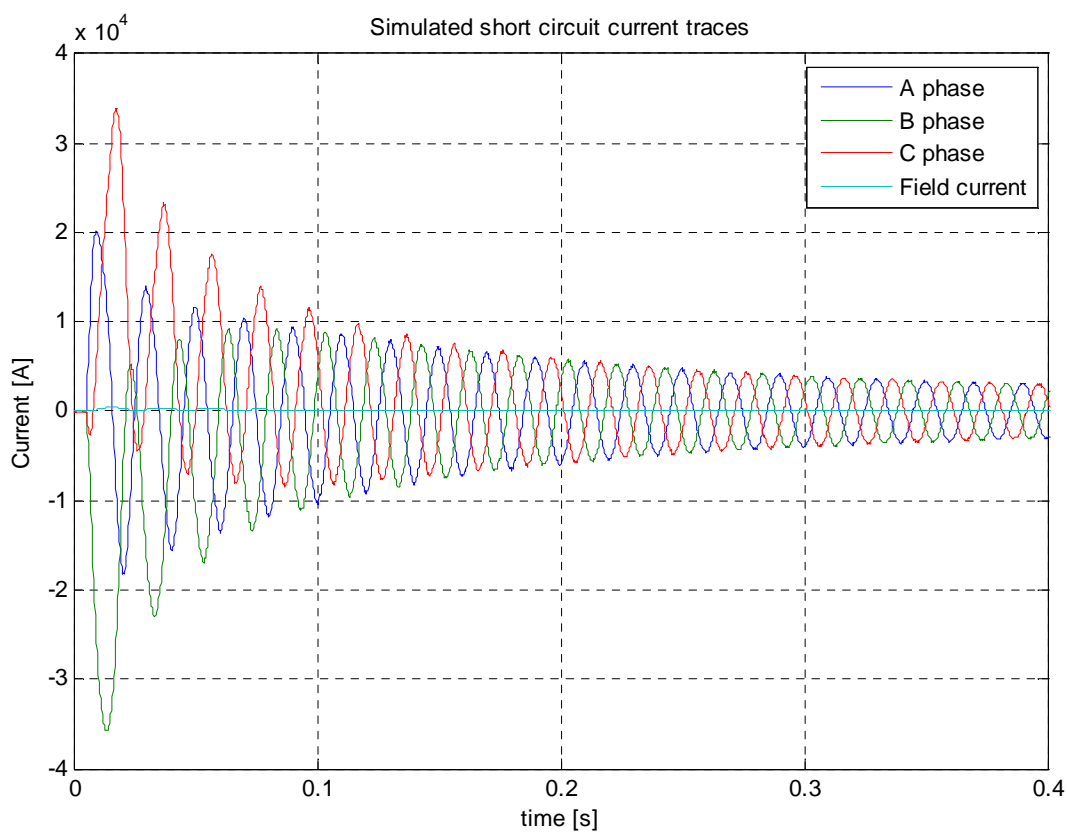


Fig. 36- Simulated short circuit current traces



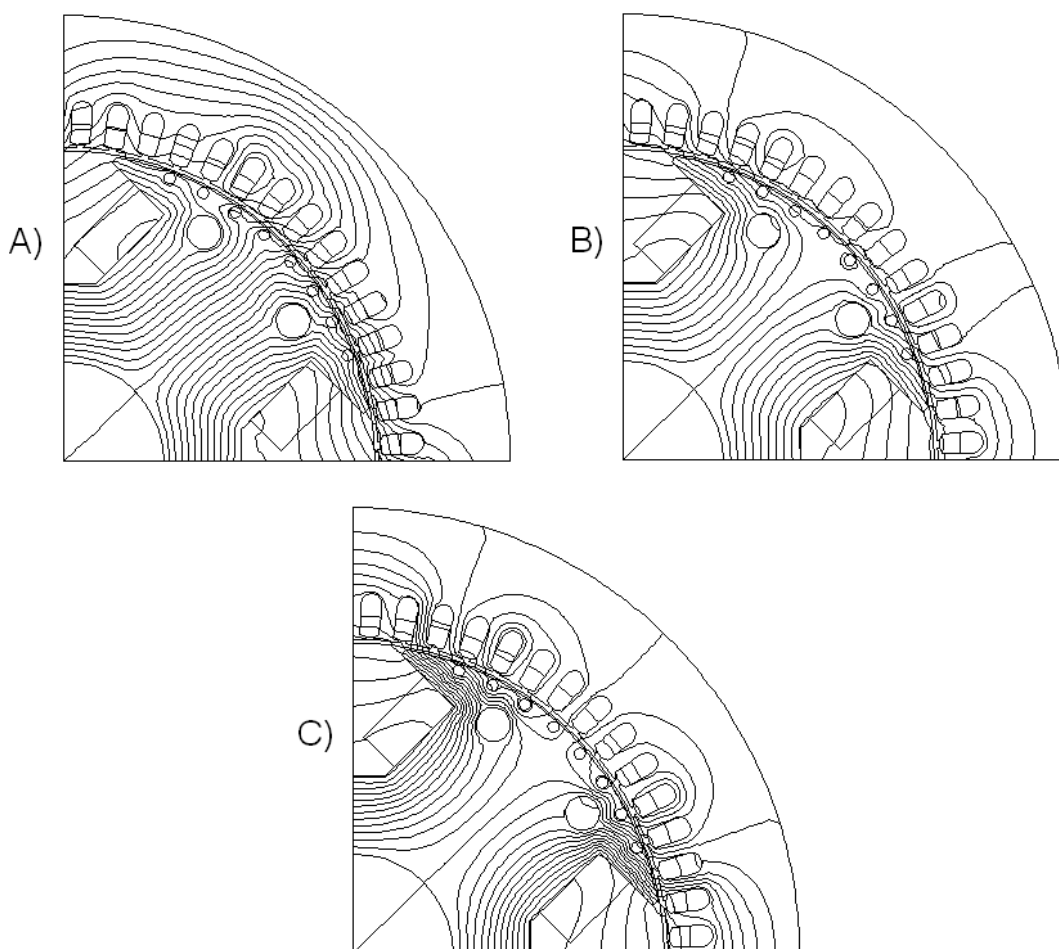


Fig. 37- Flux plots for Sudden Short Circuit simulation at different time instants after the three phase balanced short circuit, A)  $t=0.005s$ , B)  $t=0.055s$ , C)  $t=0.195s$ .

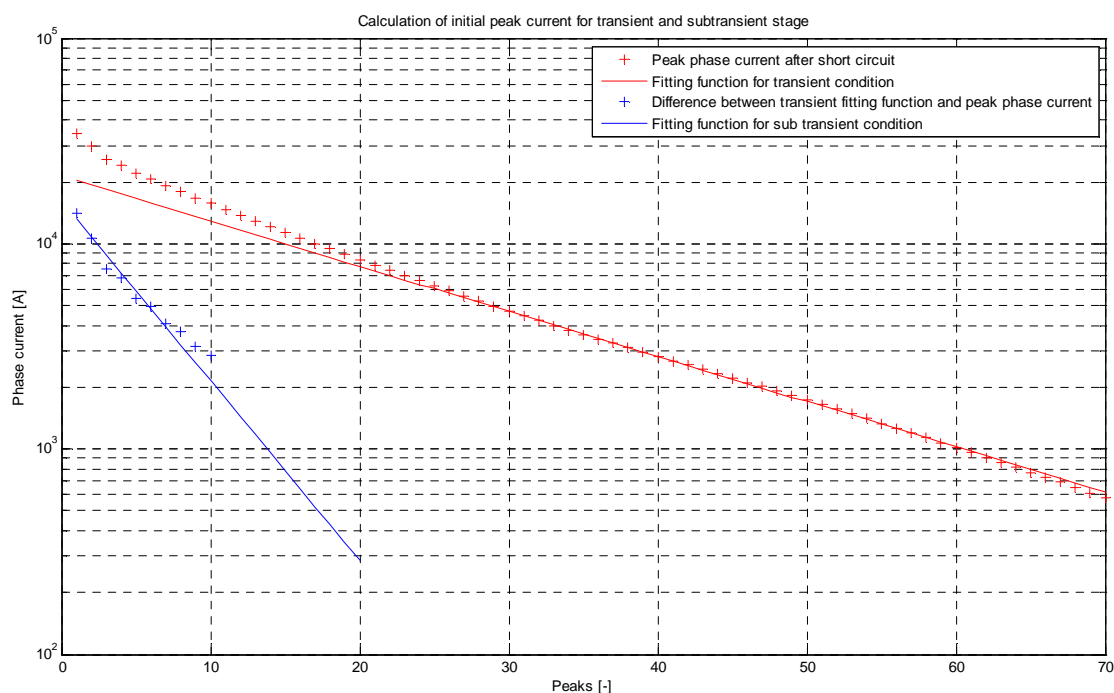


Fig. 38- Extrapolation of transient and subtransient peak current

## 8 TESTING OF SYNCHRONOUS MACHINE

Exhausting description of standard methods for testing of synchronous machine is given in [9] and also in [5]. One of these methods was used for evaluation of simulated results and will be described in following section.

### 8.1 Sudden three phase short circuit test

Sudden three phase short circuit test is one of the main standard methods for determination of transient and subtransient reactance in direct axis of the synchronous machine. Transient and subtransient reactance is obtained by analysis of an oscillogram of currents after the symmetrical three phase short circuit is applied at the machine terminals. The machine is driven at nominal speed by prime mover and terminals are open circuited. Field winding must be supplied with DC current in order to get rated open circuit voltage at the machine terminals. At chosen time instant, the short circuit is applied and current and voltage traces are recorded. Schematic diagram for this procedure is given on Fig..

Analysis of the oscillogram is straightforward and it's widely described in literature and standards. Two envelopes and mid-point curve is created for each trace. Resultant waveform is decomposed into symmetrical and unsymmetrical component and peak values of unsymmetrical component are plotted on semi-logarithmic paper. Values of transient and subtransient currents are identified by extrapolation of the curve on semi-log plot and reactances are given as a ratio of no-load voltage, before the short circuit, to the initial asymmetrical current. Usually several measurements are performed and then resultant values are computed as an average. The Short Circuit test was repeated three times and reactances were computed for each phase and each attempt.

For post-processing of measured current traces was used the same automated script as in case of FE simulation.

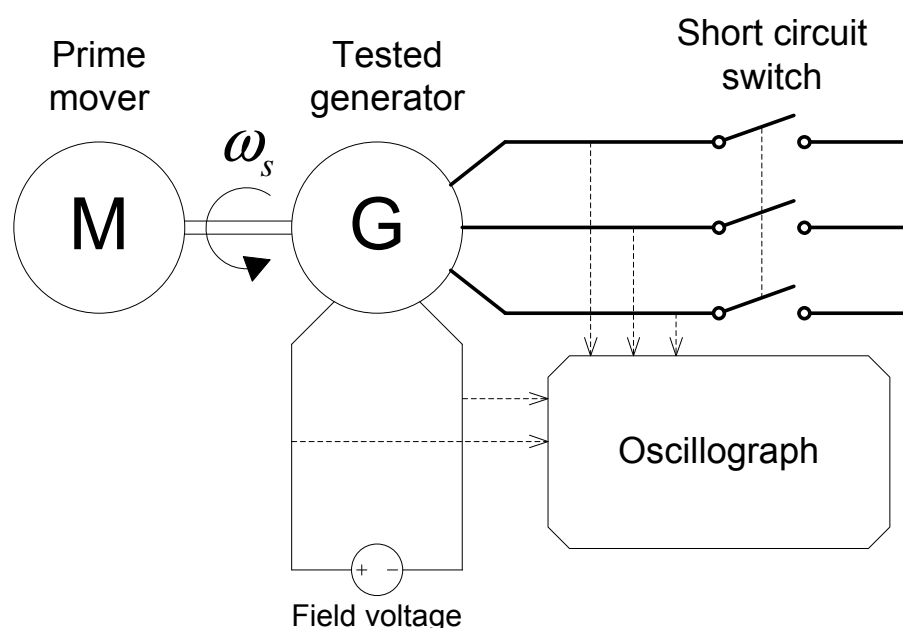


Fig. 39- Schematic diagram of sudden short circuit test

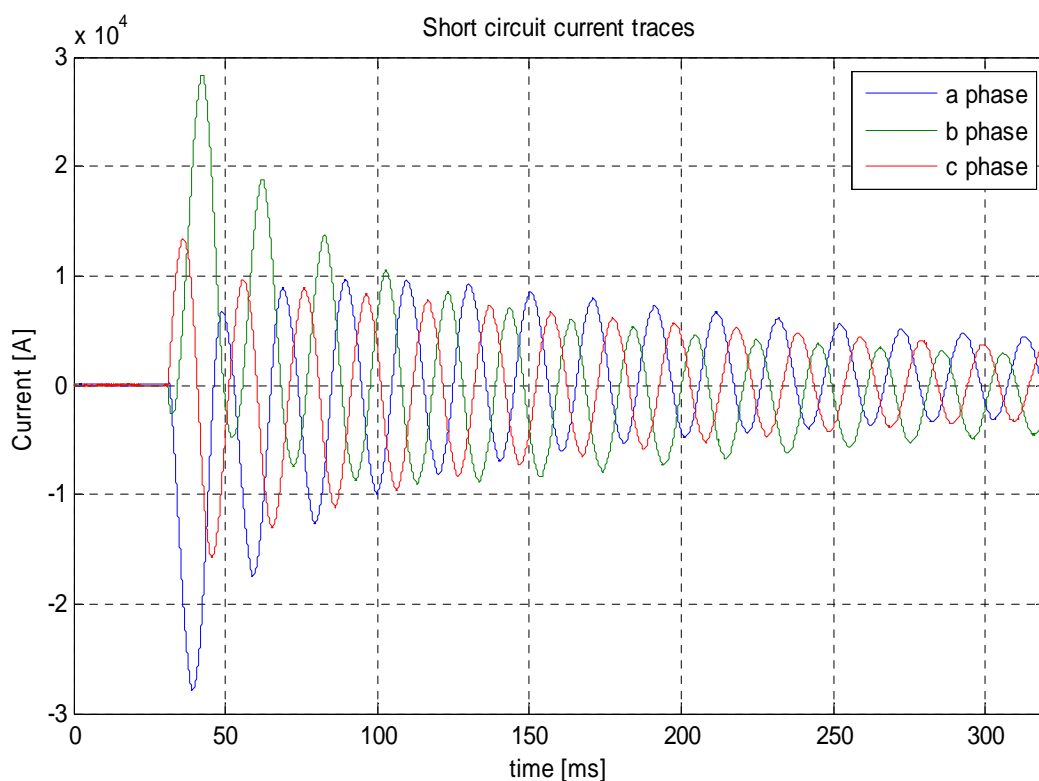


Fig. 40- Short circuit current traces during the sudden short circuit test

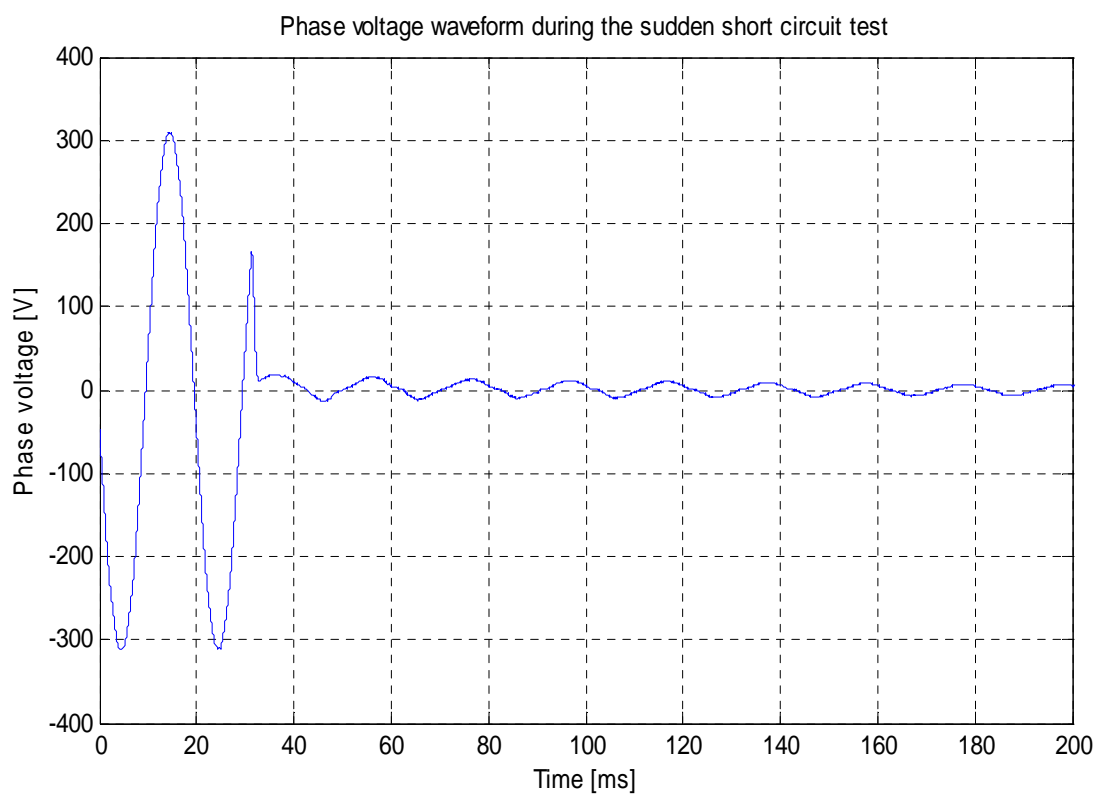


Fig. 41- Phase voltage waveform during the sudden short circuit test

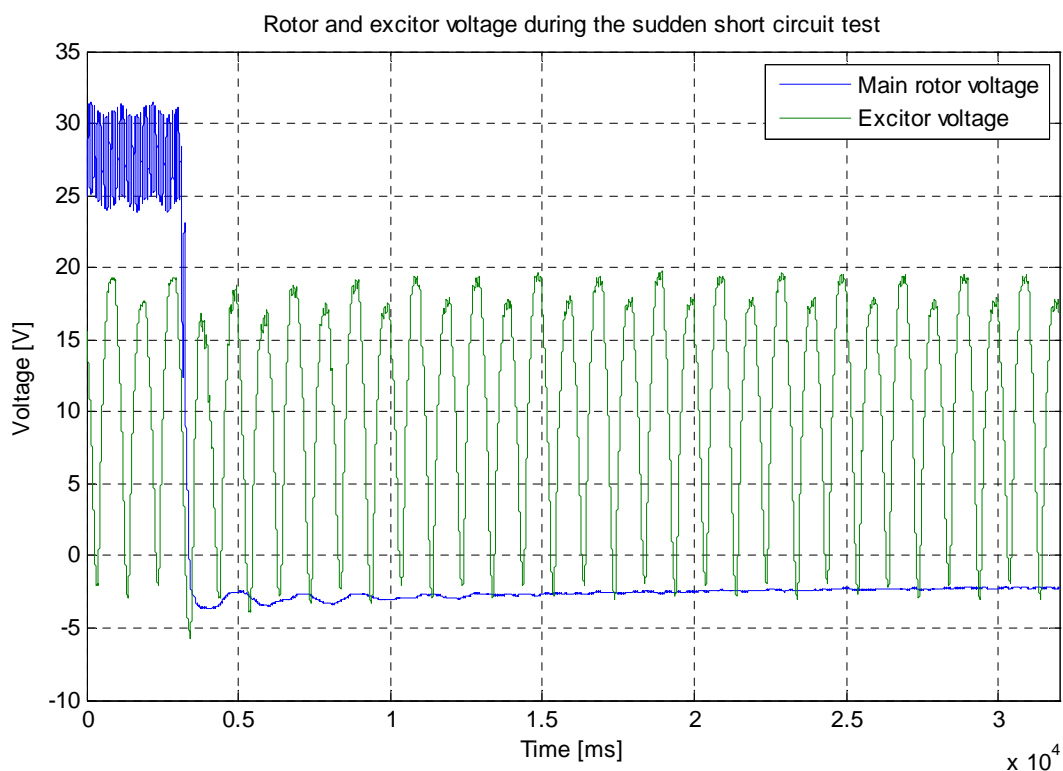


Fig. 42- Rotor and exciter voltage during the sudden short circuit test

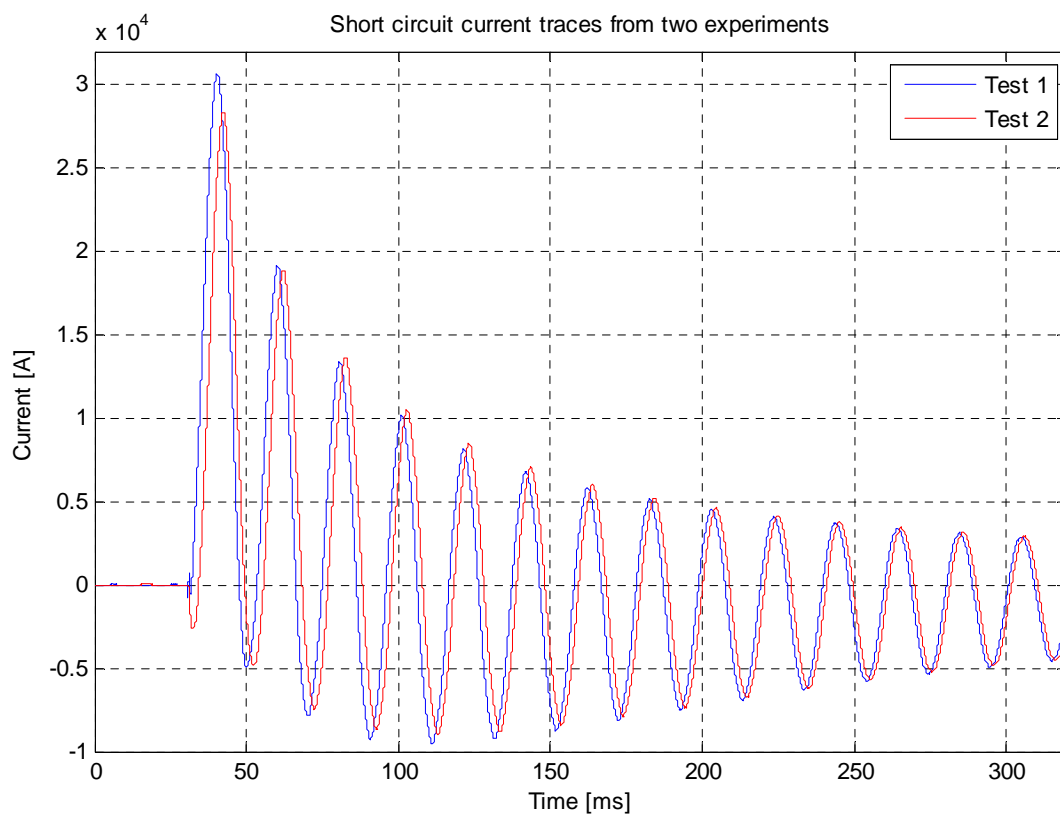
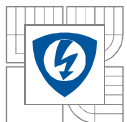


Fig. 43- Comparison of current traces from two independent Sudden Short Circuit tests



## 8.2 Test results and simulation results

This section gives an overview of results obtained by simulations and measurements. Main task was to identify these parameters:

- Direct axis synchronous reactance:  $X_d$
- Quadrature axis synchronous reactance:  $X_q$
- Direct axis transient reactance:  $X'_d$
- Direct axis subtransient reactance:  $X''_d$
- Quadrature axis subtransient reactance:  $X''_q$

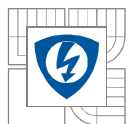
Synchronous reactances were computed with respect to the cross coupling effect and this cannot be done by test, resultant contour plots are given in chapter 6.

Summary of transient and subtransient parameters obtained by proposed procedures is given in following table:

Short circuit simulation	
$X_d'$ [p.u.]	0.2676
$X_d''$ [p.u.]	0.1503
Frequency response simulation	
$X_d''$ [p.u.]	0.1513
$X_q''$ [p.u.]	0.1404
Short circuit test	
$X_d'$ [p.u.]	0.2734
$X_d''$ [p.u.]	0.1803

*Tab. 3- Table of results*

It is apparent from Tab.3 that there is a good agreement between frequency response simulation and short circuit simulation. However, the values obtained from measured traces are higher. From the measured short circuit current traces can be observed, that peak values are lower, therefore machine is less saturated. Lower short circuit currents were probably caused by additional inductance and resistivity of cables, switchgear and measurement devices. Results obtained by magneto static and time harmonic simulations also shows a good agreement with other two simulations (end winding leakage reactance has to be added up to get comparable results), however it is impossible to chose correct value of reactance, from the reactance profile, without knowledge of peak short circuit current, thus it was concluded that sudden short circuit and frequency response simulations are more practical for analysis of unknown machine. Unfortunately, the time stepping simulation of the dead short circuit is the most time consuming method.



## 9 CONCLUSION

Primary goal of this thesis was to investigate methods for calculation of synchronous machine equivalent circuit parameters. Traditionally these parameters are obtained either by analytical calculations, based on equivalent reluctance circuit with equivalent air gap estimation, or by testing of actual machine. Another way of computation of the machine constants is by using modern numerical methods, such as Finite Element Method. In recent years there have been many advancements made in the art of FE analysis of three phase synchronous machine operation during steady state and during transients. Modern software packages, based on Finite Element Method, allow precise computation of field problems even with non-linear material properties or time variance.

Estimation of the machine constant in this thesis is divided into two parts. First part is focused on steady state operation and employs well known procedure of reactance estimation from magneto-static field solution. Synchronous reactance is defined as a ratio of flux linked with a coil and current in the coil. Magneto-static FE model is excited by chosen value of current and then flux linkage is computed from average value of magnetic vector potential distribution across the slot region. Synchronous machine is usually described by means of two reaction theory, thus reactances were computed in direct and quadrature axis using Park Transformation matrix. Impact of saturation was treated by two separate simulations. In first simulation, it was assumed that there is no magnetic interaction between the two axis of the machine. FE model was excited by pure d or q axis current, and reactance was computed for several values of currents in order to capture the reactance profile. Second simulation was carried out with combination of d and q axis current in the stator winding and the reactance was captured in a form of two dimensional matrixes for different combination of d and q axis currents. I was concluded that the matrixes may be used as a look-up table for complex dynamic model of the machine. Simulations were carried out under the assumption that the machine axial length is infinite and the machine geometry is invariant along the axial length. This assumption simplified the problem but neglected the three dimensional effects, such as end-winding leakage. End winding reactance was added to the model by analytical equation based on calculation of effective end-winding length.

Second part of the simulations was focused on estimation of transient and subtransient reactances. This is usually done by testing of the machine either by sudden short circuit test or frequency response test. It was investigated, how to mimic these methods in FE software or what other options are available. It was found in literature that there are four different methods of obtaining dynamic parameters. First method employs magneto-static solver and induced currents are replaced by equivalent boundary conditions placed on the boundaries of the current carrying areas. Advantage of this method is that, thanks to the magneto-static solver, solution is obtained immediately and post-processing of the filed solution is done in similar way as in case of synchronous reactance computation. Non-linear materials may be used and the reactances are obtained as a function of imposed current. Unfortunately without the knowledge of initial short circuit current it's difficult to choose one value representing the saturated transient or sub-transient reactance according to the standard short circuit test. Similar problem is in case of second method, which employs Time-Harmonic solver. The method use the same model as for computation of synchronous reactances but the imposed currents are harmonic. Frequency of imposed currents distinguishes the transient and subtransient operation. Fifty hertz was chosen for simulation of subtransient stage and one hertz for transient stage. These values are proposed in literature, but the results in this thesis shows that even small perturbation of input frequency may change resultant reactance significantly. Third method is called Single Frequency Response method, and it mimics the

standard IEEE procedure of obtaining subtransient reactances. This method cannot be used for computation of transient reactance but it is useful in combination with sudden short circuit method, because it allows identification of q axis subtransient reactance. The method employs time-harmonic solver with coupled external electrical circuit thus accuracy of the method is affected by parameters of external circuit, namely phase resistance and end-winding reactance. Computed values for nominal voltage and nominal frequency may be considered as saturated and error against values obtained by sudden short circuit test is within. Finally the Sudden Short Circuit was investigated. This method is traditional way of obtaining machine parameters in direct axis and its application is widely described in literature. Simulation was carried out by using time-stepping solver coupled with external electrical circuits and reactances are obtained by post-processing of short circuit current traces. Main disadvantage of this method is the long computation time and potential errors during exponential fitting of the peak current traces on semi log plot. Automated Matlab script was developed in order to get precise curve fitting and more accurate results. Inputs of the script are current traces in each phase and output is average value of transient and subtransient reactance in direct axis. It was concluded that due to the complicated curve fitting in the subtransient part of the current trace, frequency response method would be more accurate. Proposed procedure for calculation of the machine constants by FE is given on Fig.43. The procedure was automated in many parts by using Matlab scripts and command files.

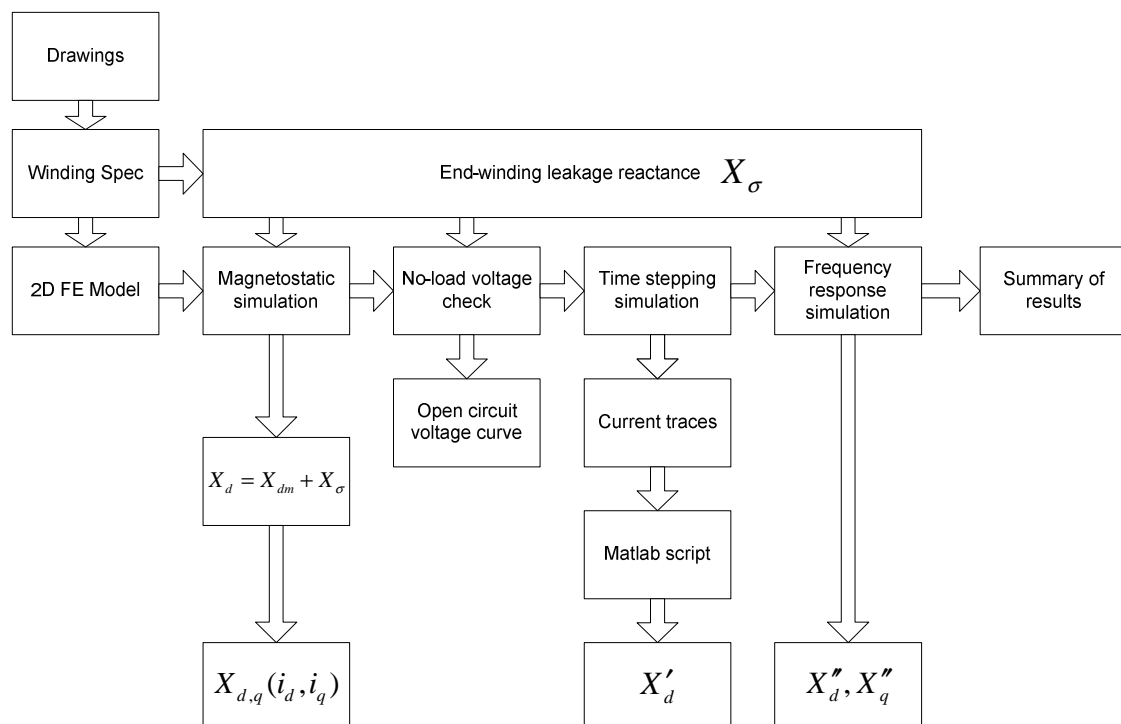
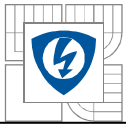


Fig. 44- Proposed simulation procedure for identification of all equivalent circuit parameters

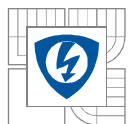
Finally a Sudden Short Circuit test was performed on actual machine. From short circuit current traces is apparent, that the actual peak current is smaller than simulated one. This is caused by additional reactance and resistance of the machine winding and measurement apparatus. This also shows the importance of external circuit's parameters prediction in coupled analysis.



Proposed methodology presents good reference for development of automated calculation tool, which will be a subject of future work. Several other topics will be investigated:

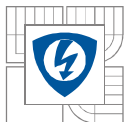
- Investigation of end-winding leakage reactance prediction using FE analysis and comparison with different analytical methods. As it was mentioned before, parameters of external circuits in two-dimensional coupled analysis have major impact on accuracy of analysis, thus precise identification is of major concern.
- Investigation of Stand Still Frequency Response method for prediction of operational parameters. This method is one of the standard methods described by IEEE standard and its application in FE analysis may bring several benefits against Sudden Short Circuit simulation, however, the suitability has to be investigated and compared with other methods.
- Further automation of the analysis procedure. Main goal is to develop application with parametric geometry interface of the analyzed machine so that the geometry is generated according to the input dimensions and standard test are then performed.
- Further measurements on actual machines and comparison against simulations.



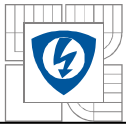


## REFERENCES

- [1] Bianchi N., “*Electrical Machine Analysis Using Finite Elements*”, CRC Press, 2005, ISBN 978-0849333996.
- [2] A.B.J. Reece, T.W. Preston, “*Finite Element Methods in Electrical Power Engineering*”, Oxford University Press, ISBN: 978-0-19-856504-8, 2000.
- [3] Sheppard J. “*Finite Element Analysis of Electrical Machines*”, Springer, ISBN: 978-0-7923-9594-2, 1995.
- [4] Juha Pyrhönen, Tapani Jokinen, Valéria Hrabovcová, “*Design of Rotating Electrical Machines*”, John Wiley & Sons, Ltd. 2008.
- [5] Ion Boldea, “*Electric Generators Handbook*”, CRC Press, 2005, ISBN: 084935725X.
- [6] Jan Machowski, Janusz W. Bialek, James R. Bumby, “*Power System Dynamics: Stability and Control*”, John Wiley & Sons Ltd, 2008, ISBN 978-0-470-72558-0.
- [7] Arie L. Shenkman, “*Transient Analysis of Electric Power Circuits Handbook*”, Springer, 2005, ISBN 0387287973.
- [8] David J. Griffiths, “*Introduction to Electrodynamics: Third edition*”, Prentice Hall, 1999, ISBN 0-13-805326-X.
- [9] Sherwin H. Wright, “*Determination of Synchronous Machine Constants by Test*”, Transaction A.I.E.E.
- [10] C.N. Ashtiani, D.A. Lowther, “*Simulation of the Transient and Subtransient Reactances of a Large Hydrogenerator by Finite Elements*”. IEEE Transaction on Power Apparatus and Systems, Vol. PAS-103, No.7, July 1984.
- [11] Silvio I. Nabeta, Albert Foggia, Jean-Louis Coulomb and Gilbert Reyne, “*A Non-Linear Time-Stepped Finite element simulation of a Symmetrical Short-Circuit in a Synchronous Machine*”, IEEE Transaction on Magnetics, Vol. 31, No. 3, May 1995.
- [12] Kolondzovski Zlatko, “*Evaluation of Methods for Calculation Synchronous Generator Reactances*”, International PhD Seminar: Computation of Electromagnetic Fields, 23-28 September 2004, Budva/Serbia & Montenegro
- [13] Drago Ban, Damir Zarko, Zlatko Maljkovic, “*The Analysis of Saturated Reactances of the 247 MVA Turbogenerator by Using the Finite Element Method*”.



- [14] Prof. JJ. Simond and colective, “*Automatic Determination of Laminated Salient-Pole Synchronous Machines parameters Based on the Finite Element Method*”, Swiss Federal Institute of Technology, Electrical Engineering Department.
  
- [15] D.Y.Park, H.C.Karmaker, G.E.Dawson, A.R. Eastham, “*Standstill Frequency Response Testing and Modeling of salient-pole Synchronous machines*”, Queens University, Canada,, IEEE transaction on Energy Conversion, Vol.13,No.3, September 1998.

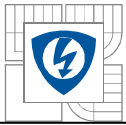


## SUPPLEMENT

[1] Matlab script for calculation of transient reactance from short circuit current traces

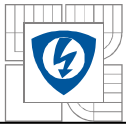
```
% Calculation of transient and subtransient reactance from
% short circuit current traces

for q=1:3
    for i=1:length(t)
        x(i)=trace(i,q);
    end
    figure;
    plot(t,x);
    [maxtab, mintab] = peakdet(x, 500, t);
    hold on;
    plot(mintab(:,1), mintab(:,2), 'g*');
    plot(maxtab(:,1), maxtab(:,2), 'r*');
    hold off
    if q==1
        for i=2:(length(maxtab)-1)
            PeakPos(i-1)=maxtab(i,2)+(-1)*(mintab(i-1,2)+mintab(i,2))/2;
            PeakNeg(i-1)=(-1)*((mintab(i-1,2)+(-1)*(maxtab(i-1,2)+maxtab(i,2))/2));
        end
        j=1;
        for p=1:length(maxtab)-2
            lines(p+j)=PeakPos(p);
            j=j+1;
        end
        p=0;
        j=0;
        for p=1:length(maxtab)-2
            lines(p+j)=PeakNeg(p);
            j=j+1;
        end
        elseif q==2
        for i=2:(length(maxtab)-1)
            PeakPos(i-1)=maxtab(i,2)+(-1)*(mintab(i-1,2)+mintab(i,2))/2;
            PeakNeg(i-1)=(-1)*((mintab(i,2)+(-1)*(maxtab(i,2)+maxtab(i+1,2))/2));
        end
        j=0;
        for p=1:length(maxtab)-2
            lines(p+j)=PeakPos(p);
            j=j+1;
        end
        p=0;
        j=1;
        for p=1:length(maxtab)-2
            lines(p+j)=PeakNeg(p);
            j=j+1;
        end
        else
        for i=2:(length(maxtab)-1)
            PeakPos(i-1)=maxtab(i,2)+(-1)*(mintab(i-1,2)+mintab(i,2))/2;
            PeakNeg(i-1)=(-1)*((mintab(i,2)+(-1)*(maxtab(i,2)+maxtab(i+1,2))/2));
        end
        j=0;
        for p=1:length(mintab)-2
            lines(p+j)=PeakPos(p);
            j=j+1;
        end
        p=0;
        j=1;
        for p=1:length(mintab)-2
            lines(p+j)=PeakNeg(p);
            j=j+1;
        end
    end
end
```



```
end
i=0;
for i=30:length(lines)-26
    difL(i-29)=lines(i)-lines(94);
    peaks(i-29)=i;
end
for i=1:length(lines)-26
    difLF(i)=lines(i)-lines(94);
    peaksF(i)=i;
end
hold off
[estimates, model] = fit(peaks,difL);
figure;
semilogy(peaksF, difLF, '*')
hold on
[sse, FittedCurve,A,lambda] = model(estimates);
for i=1:length(peaksF)
    curveB(i) = A.*exp(-lambda * peaksF(i));
end
semilogy(peaksF, curveB, 'r')
xlabel('peaks')
ylabel('f(estimates,xdata)')
title('Fitting to function ');
Vpp=620;
iss=lines(94);
t0=A*exp(-lambda *(1-0.607));
XdTran(q)=Vpp/(t0+iss);
for i=1:10
    peaksC(i)=i;
    curveC(i)=difLF(i)-curveB(i);
end
semilogy(peaksC,curveC,'*');
[estimatesC, model] = Fitc(peaksC,curveC);
[sseC, FittedCurveC,Ac,lambdaC] = model(estimatesC);
for i=1:20
    curveClin(i) = Ac.*exp(-lambdaC * peaksF(i));
    peaksClin(i)=i;
end
semilogy(peaksClin, curveClin, 'g')
t0stripe=Ac*exp(-lambdaC *(1-0.607));
Xdsub(q)=Vpp/(t0stripe+t0+iss);

hold off
end
```



### [2] Peak detection function

```
function [maxtab, mintab]=peakdet(v, delta, x)

maxtab = [];
mintab = [];

mn = Inf; mx = -Inf;
mnpos = NaN; mxpos = NaN;

lookformax = 1;

for i=1:length(v)
    this = v(i);
    if this > mx, mx = this; mxpos = x(i); end
    if this < mn, mn = this; mnpos = x(i); end

    if lookformax
        if this < mx-delta
            maxtab = [maxtab ; mxpos mx];
            mn = this; mnpos = x(i);
            lookformax = 0;
        end
    else
        if this > mn+delta
            mintab = [mintab ; mnpos mn];
            mx = this; mxpos = x(i);
            lookformax = 1;
        end
    end
end
end
```

### [3] Function for exponential curve fitting

```
function [estimates, model] = fitcurve(peaks, difL)
start_point = rand(1, 2);
model = @expfun;
estimates = fminsearch(model, start_point);
    function [sse, FittedCurve,A,lambda] = expfun(params)
        A = params(1);
        lambda = params(2);
        FittedCurve = A .* exp(-lambda * peaks);
        ErrorVector = FittedCurve - difL;
        sse = sum(ErrorVector .^ 2);
    end
end
```

[4] Magnetization curve for M470-65 laminations of analyzed machine

